Photocatalysis Using Semi-Conducting Polymers for Wastewater Treatment

Author: Ellie McBurney
Supervisor: Dr Alisyn Nedoma
Department: Chemical and Materials Engineering

Acknowledgements

I would like to sincerely thank the following for their contribution to this research project:

Rahul Kumar
Doctoral Candidate – Civil and Environmental Engineering

for his unwavering assistance, lab and life advice, and for always putting in the UV lamps.

Dr Lokesh Padhye
Department of Civil and Environmental Engineering

for providing research focus and drive, a beautiful laboratory and unfailing encouragement.

Asith Gunaratna and Pramodi Jayananda
Part IV Civil and Environmental Engineering Students; a.k.a Team PEDOT

for being the best-ever lab partners, the fastest UV-Vis measurers, and neatest labellers.

&

Dr Alisyn Nedoma
Department of Chemical and Materials Engineering

for providing the best explanations and encouragement, making the strongest coffee I've ever tried, and for consistently affirming and reminding me of my own abilities.

Abstract

The following research has investigated photocatalysis using the semi-conducting polymers poly(3,4)ethylenedioxythiophene (PEDOT) and polyaniline (PANI), as a potential technology for the treatment of organic contaminants in wastewater. First, the complex problem environment of failing water treatment technologies in the developing world has been established, reflected in the high rates of disease and deaths due to water related risk factors. Next, the universal nature of water quality issues has been explored, with emerging contaminants of concern and pharmaceutical bioaccumulation in aquatic environments highlighted as parallel and similarly complex issues. Three photocatalysis have been chosen to explore polymer performance and provide comparison with current standards: PEDOT, PANI, and Zinc Oxide (ZnO) nanopowders. All catalysts have been tested under UVA light for their photocatalytic abilities to degrade methylene blue (MB) dye. While PEDOT has shown superior adsorption and photocatalytic properties, PANI has proven to be underwhelming in every category. PEDOT has presented with a power-law Bangham kinetics model of adsorption, degrading 44% MB in dark conditions after 60 minutes. With UV exposure, PEDOT has achieved 88% degradation MB under UVA conditions and 100% under the higher energy UVC after 60 minutes exposure, and results have also suggested there is an integrated relationship between adsorption and photocatalysis with higher adsorption appearing to lead to ‘rapid-onset’ photocatalysis. Photocatalytic degradation of MB with PEDOT has been shown to favour basic conditions, potentially due to higher number of hydroxyl species available to be oxidised into hydroxyl radical species. ZnO has performed exceptionally under UVA exposure, completely degrading MB dye within 30 minutes, and, as expected, showing no adsorption abilities under dark conditions. Mixtures of polymer and ZnO at different mass fractions of ZnO have been successful at completely degrading MB dye after 30 minutes, highlighting polymer/ZnO composites as a promising avenue for further research.

Table of Contents

Table of Figures

Introduction & Project Background

I. Introduction

Water access and availability is one of the major issues facing our world, and will become an even bigger problem in the coming years. Unfortunately, as with many complex issues, water availability (or the lack thereof) intersects with many other ecological and societal issues, including climate change, point and non-point source pollution, and poverty [1]–[5]. Of particular concern are the high rates of water related illnesses and diseases. In 2000, around 2 billion deaths due to diarrheal diseases were attributed to the 'water and sanitation' risk factor, with 90% of cases among children under five [2]. In 2015, the United Nations (UN) released the Sustainable Development Goals, a set of 17 goals to end poverty, tackle climate change, and "ensure prosperity for all" [6]. Goal Six, titled "Clean Water and Sanitation" is dedicated to this pressing problem, and is noted by the UN and others to be an extremely important goal that is heavily integrated into the success of other goals [4], [7], [8]. In the 2016 Global Sustainable Development Report, the UN highlighted the impact that infrastructure has on inequality, and the large impact that both these factors have on the resilience of communities, with 663 million people lacking access to clean water and 2.4 billion lacking access to sanitation in 2016 [7]. It is clear that without easily accessible water for drinking, cleaning, cooking and sanitation purposes, communities living in poverty struggle to improve their circumstances. Furthermore, by 2025 it is estimated that two thirds of the world's population will live in water stressed countries [9], confirming without doubt that water supply and treatment is an issue concerning all people.

For many of the Sustainable Development Goals, science and technical development has been presented as a tool toward their achievement, along with carefully considered management approaches [6], [10], [11]. The successful yet large and costly treatment processes used in developed countries such as New Zealand, [12] however, struggle to be implemented in the developing world [8], [13]. The World Water Development Report (2017) highlights the high operations and maintenance costs required for membrane based systems, for example, such as reverse osmosis and filtration which is commonly used here [14]. A new solution, therefore, is required. The 2017 report suggests a route of enquiry for this new solution by highlighting a secondary problem: emerging contaminants [14]. These include pharmaceutical products and metabolites, as well as the emergence of endocrine-disrupting compounds. There is a strong

argument that developing a process with multiple applications can increase system resilience [1], [3], [14], thus, a process that can both remove these emerging contaminants and answer to water scarcity and availability issues is firmly set as an idealised benchmark to reach. The report specifies “chemically advanced oxidation” [14] as a method able to remove emerging contaminants, with one such advanced oxidation process being photocatalysis [15]–[19]. Photocatalysis has therefore been chosen as the focus of this research due to its superior ability to degrade both trace amounts of emerging contaminants, such as pharmaceuticals [19], [20], and the as-yet not fully developed potential to degrade pathogens under visible light [21]–[23].

II. Pharmaceuticals and Emerging Contaminants

Ohko *et al.* (2002) succinctly state the effects that natural and synthetic estrogens are having on the aquatic environment, and the large threat this could potentially contain for humans [17]. They state that “abnormal sexual development in animals" are widely reported, and argue that this is due to estrogens and chemicals with estrogenic activity that are not removed during the water treatment process and are instead released into the ocean. Moreira *et al.* (2016) support this position, and go further to place contaminants of emerging concern, such as estrogen and other endocrine disrupting substances, in the same category as antibiotic resistant bacteria with regards to the threat posed to human health [24].

Ebele, Abdallah and Harrad highlight the damaging effect of Personal Care Products (PCPs) on the freshwater aquatic environment, due to their persistence and subsequent bioaccumulation and toxicity [20]. Bioaccumulation, rightly so, is argued as a pressing issue due to the presence in the environment of PCPs and the accumulation of metabolites over time which remain biologically active and impact aquatic organisms, in similar ways to estrogen. Toxicity arises as many pharmaceuticals were designed to maximise biological activity at low concentrations, and to target specific metabolic, enzymatic, or cell-signalling mechanisms. Thus their impact is large even in small concentrations within the aquatic environment and the water cycle [20]. In this research, the dye methylene blue (MB) has been used as a model for organic pollutants within the environment: both trace pharmaceutics and other pollutants such as pathogens and bacteria.

III. Photocatalysis

While the main source of emerging contaminants comes from municipal sewage and treated wastewater [24], according to the United Nations World Water Development Report (2018), it is estimated that 80% of all industrial and municipal wastewater are released to the environment without any treatment at all [3]. This is an alarming statistic, and highlights that the current method adopted in the developed world is not and ca not be easily translated to less developed regions. Prieto-Rodriguez *et al.* highlight the benefit of Advanced Oxidation Processes (AOPs) as valuable methods for degrading persistent organic compounds. This is due to non-selective hydroxyl radicals that are able to promote organic matter oxidation at high reaction rates [15]. One such method is photocatalysis [15], [17], [19]. Photocatalysis occurs via the schematic below, with photons from incident light activating electrons from the valence band into the conduction band, thus having the ability to react with oxygen (O_2) and hydroxyl (OH^-) species present within the water, creating extremely reactive free radical species.

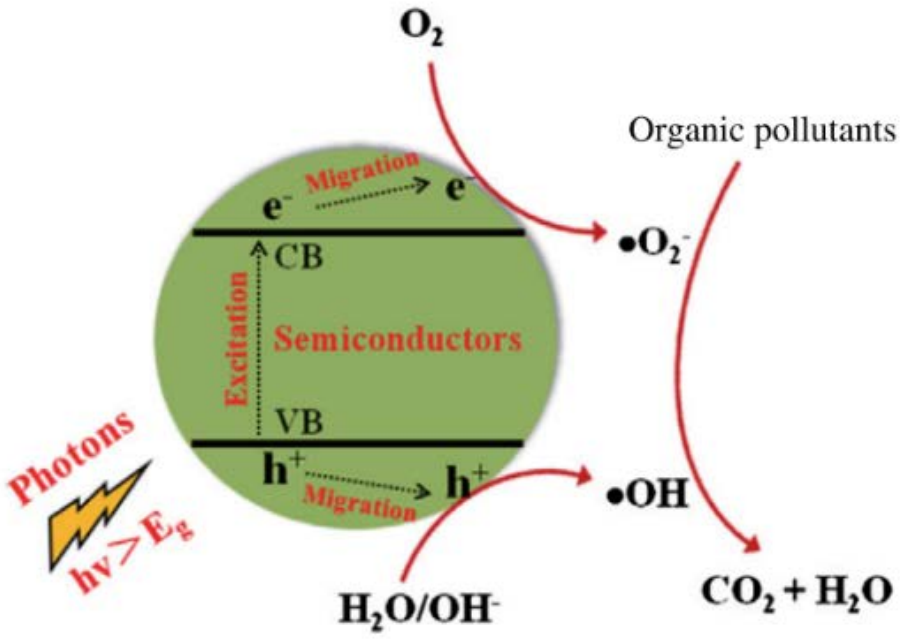

Figure 1: Schematic of the photocatalysis process from Wang et al (2015) [25].

A. Metal Oxides: The Benchmark

Metal oxides such as titanium dioxide and zinc oxide are currently considered the best materials for photocatalysis, due to their reliability, high chemical stability and relatively low price [15], [16], [23], [25]. Moreira *et al*'s 2015 study highlighted TiO_2 coated glass Rashig rings with LEDs irradiation was the most efficient for the removal of emerging contaminants from urban wastewater [24]. Although this study involved photocatalytic ozonation as opposed to UV light activation, the underlying principle of using a metal oxide for photocatalysis remains the same. Metal Oxide catalysts require UV light activation due to their large band gap [16], [23], and designing sunlight driven photocatalytic reactors face large challenges, as Wang et al explore in their review of the photocatalysis space from 2015 [26]. There is a gap in knowledge regarding the definitive design for a reactor and catalyst combination that may be able to answer to these issues. Wang *et al* suggest the method of creating non-UV catalysed materials begins with investigating doped-TiO2 systems, and continues by investigating further into non-TiO2 based photocatalysis, and clearly explain the method of photocatalysis involving the excitation of semiconductors followed by the separation of electron-hole pairs [27].

B. PEDOT

PEDOT poly(3,4ethylenedioxythiophene) became popular during the 1990s, going from no mentions in a paper in 1990 to sixty five papers written in the year 1999 about this promising semiconducting polymer [28]. The semi-conducting nature of PEDOT occurs in a similar fashion to the metal oxides, with electrons excited into the conduction band from the valence band. In the case of polymers, however, the chain structures then facilitate the conduction of electricity down its length [16]. In 2015, Ghosh *et al* published a paper detailing the “superior" polymer nanostructure of PEDOT, wherein they synthesised spindles of polymer which can be activated by visible light and is “one of the most promising conjugated polymers with a wide range of applications" [21]. The paper finds a band gap of 1.69eV, and that the photocatalytic activity of PEDOT is shape dependent but also robust, with activity retained over six successive experimental runs at least 95% of the initial activity. While Ghosh's paper details a complicated method of synthesising PEDOT which will not be covered in this research, the main synthesis is the same, occurring via oxidation of the monomer, EDOT, with ferric chloride, to catalyse the polymerisation and form PEDOT.

Shi *et al.* highlight an alternative method for synthesis of PEDOT, using anions to promote self-inhibited polymerisation of the polymer. They first compare the somewhat easier route of synthesising PEDOT with a polystyrene backbone makes it soluble (PEDOT:PSS). However, this conjugate is semi-soluble in water and a non-soluble version for water treatment application[29] is preferred [29]. Shi *et al*. suggest that doping pure PEDOT with some sized anions (S-PEDOT) will lead to a material with a greater potential for electrical applications because of their compact and ordered polycrystalline structure [29]. This means they have better electrical conductivity and Seeback coefficient, although the high quality films can often be hard to make as the polymerisation process is not easily controlled. While PEDOT films are a promising avenue, both Ghosh and Shi have highlighted the versatility of this polymer and present some good improvements in polymer activity. This research aims to explore activity and conditions of polymer-based photocatalysis by testing the hypothesis presented by these authors that semi-conducting polymers are effective photocatalysts, with polymer structure an important yet secondary consideration to the photocatalysis achieved.

C. PANI

Polyaniline (PANI) is also considered a promising photocatalyst, with research managing to activate PANI using the visible light spectrum [30]–[33]. Gilja *et al.* (2017) consider in particular the synergistic effects of Polyaniline/TiO_2 systems for the degradation of dyes in wastewater, and present findings that show PANI as a high quality photocatalyst when part of a composite with other species [34]. Whilst their findings are encouraging, and supported with similar visible light activated results from other authors [30], [31], there are concerns regarding the time taken for photocatalysis, and also questions surrounding the methods of synthesis that call into question the validity of the results. Although PANI is therefore a promising catalyst, it has much to prove in the field of wastewater treatment, which this research attempts to further investigate.

Materials & Methods

See appendices for all safety data sheets, HAZOP and product information. All materials purchased from Sigma Aldrich / Merck.

IV. PEDOT synthesis:

A. Materials & Apparatus:

EDOT monomer, $FeCl_3$, Water, Methanol (for rinsing). All materials reagent grade from Sigma Aldrich. Apparatus of note include water bath with heated stirring pad, and vacuum pump filter seen to the right.

Figure 3: Water Bath

Figure 2: Vacuum Pump Filter

B. Method:

The first step in creating PEDOT was to prepare the water bath by filling the metal bowl with water and covering with aluminium foil for insulation. The apparatus pictured was the best for this process as it was attached with a thermometer. The bath was set to reach 50°C and typically took half an hour to reach the set point.

Meanwhile, a 1.5M aqueous solution of ferric chloride was prepared by measuring 2.415 g of ferric chloride powder. Care was taken by placing aluminium foil on the bench prior to weighing with the balance, due to the rapid oxidation of the powder and the high probability of staining the bench. Standard laboratory practice of measuring in small glass vials also helped to avoid spills and increased measurement reliability.

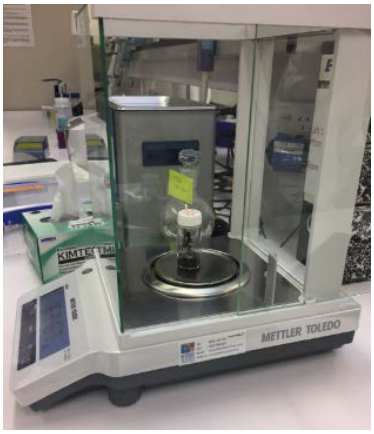

Figure 4: Measuring ferric chloride in glass vial.

Next, 10mL of distilled water was measured into a measuring cylinder and added to the vial of ferric chloride. The vial warmed upon mixing, as was expected with the acid-base exothermic reaction happening upon hydration of the ferric chloride. This was then stirred whilst covered with foil for 20 minutes. Next, 2 g of EDOT monomer (~1.5mL) was measured, using a pipette, and added into the same vial. This was attached to the clamp stand on the water bath and stirred for 30 minutes at 50°C. This vial was then left overnight to polymerise fully.

The vial then became a dark colour as the PEDOT polymer powder had precipitated out of solution. To extract the polymer powder, vial contents were washed through with methanol in the vacuum pump filter, as seen in Figure X. The black powder was then scraped off the 0.45 µm pore nylon filter paper and was left overnight to air-dry under the fume hood.

Figure 5: Thick layer of PEDOT powder sitting on vacuum pump filter following filtration. Spent yellow filtrate solution can be seen in the bottom of the flask.

The original method inherited from Thomas Kerr-Phillips required 500mg of EDOT monomer, however this was increased first to 1 g and subsequently 2 g, to increase PEDOT yield. Polymerisation time was also increased to ~24 hours to account for this increase, otherwise monomer remained in solution and was filtered out. If the PEDOT unfiltered vial still has a distinct odour, then the polymerisation has not completed. In some cases the spent filtrate solution was observed to continue polymerising, suggesting that the exact amounts of monomer and oxidant in this reaction are yet to be optimised and require future work.

V. PANI Synthesis:

A. Materials & Apparatus:

Aniline, diethylene glycol, APS, water. All materials from Sigma Aldrich. No heating required. Aniline monomer is highly toxic when in high concentrations, vacuum pump also required as for PEDOT.

B. Method:

PANI synthesis was carried out at all times under the fume hood due to the toxic nature of aniline monomer. The following synthesis method was adapted from Eskizeybek *et al.* (2012) [31]. 0.4M aniline monomer was prepared with 1M diethylene glycol. At the same time, 0.4M APS was added to another 1M solution of diethylene glycol. The APS/diethylene glycol solution was then added dropwise to the aniline/diethylene glycol solution while it was stirred continuously, a process taking at least 20 minutes. The APS solution first presented as a colourless solution, while the aniline solution once properly mixed was orange and darkened to dark green as the PANI powder precipitated out, as can be seen in Figure 6 and Figure 7 below.

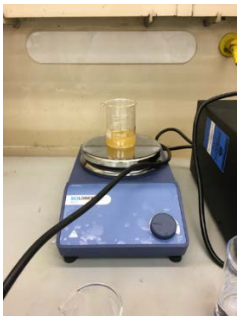

Figure 6: Aniline and diethylene glycol solution. Stirred under the fume hood to avoid excessive inhalation, important due to the safety concerns regarding over-exposure to aniline. Stirring with diethylene glycol rapidly mixed the previously immiscible components.

Figure 8: Precipitated PANI powder darkening beaker. Labels showing name, date and contents were essential to ensure safe laboratory processes.

Figure 7: Aniline monomer in water prior to addition into diethylene glycol solution. Interestingly, aniline appears insoluble in water until the addition of the diethylene glycol and subsequent stirring, at which time the solution turns a light orange colour.

To increase the ease of preparation, the method was adapted. Each reactant was first added to 10mL measuring flasks, such as the one to the right. This required 0.365mL aniline and 0.947mL diethylene glycol measured using a pipette, to reach 0.4M and 1M respectively. 0.912 g APS was measured out on the balance and also added into a 10mL measuring flask to achieve a 0.4M aqueous solution. Two small beakers, one containing aniline and diethylene glycol, and one containing APS and diethylene glycol were then created, with the APS solution subsequently added dropwise into the aniline solution as it was stirred.

The final beaker of PANI was left overnight to ensure sufficient polymerisation, and was then filtered and dried in a similar manner as PEDOT. It was washed through with water instead of methanol and subsequently took longer to air-dry.

Figure 9: Synthesised PEDOT (left) and PANI (right) powders following drying and weighing of 20mg. Static on the weigh boats can be clearly seen. It was soon discovered that glass vials were much better than boats due to their lack of static electricity and better reliability of results.

VI. UV Experimental Method:

A. Materials & Apparatus:

The UV experiments involved the degradation of methylene blue (MB) dye in the UV chamber. MB first presents as a dark green powder. We created stock solutions of 32mgL^{-1} of the blue dye to streamline lab work and also to keep the base solution for each set of experiments consistent. At the start of each lab session MB dye standards were measured, to be used during calibration of the UV-Vis spectrophotometer which would be used to measure concentration results. Meanwhile, catalyst samples (PEDOT, PANI or ZnO) were weighed out into small vials, taking into account triplicate measurement requirements and usually requiring 25mg in each vial in order to create 1gL^{-1} solutions.

The sample bottles to record samples were also labelled during this preparation time, as some experiments generated 45 samples it was imperative to keep track of samples effectively. The layout of the labelled bottles can be seen in the figures below.

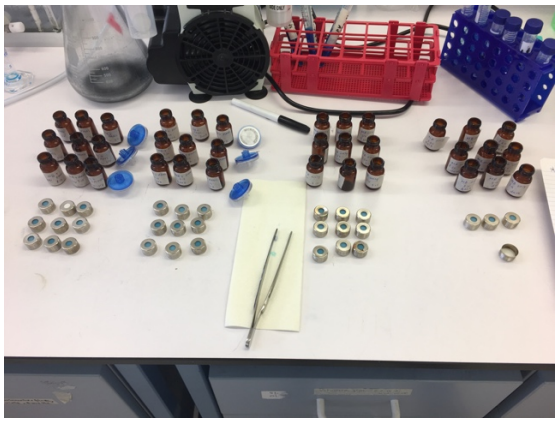

Figure 10: Experimental Layout

To begin the experiment, the adsorption phase began first with 30 minutes of stirring in dark conditions. This was achieved by covering the beakers in aluminium foil, as seen to the in the image to the left.

Figure 11: Adsorption Phase

Following 30 minutes of adsorption, half of the samples were then placed in the UV chamber, usually with all 8 UVA lamps installed. The UV treatment phase was then completed for either 30 or 60 minutes, with samples taken at certain intervals and stored in the previously labelled bottles, ready for measurement on the UV-Vis machine.

Figure 12: Placing beakers into the UV chamber.

Figure 13: Beakers post-UV treatment, blue MB dye colour has disappeared to leave colourless solution with dark polymer powder.

The UV-Vis machine required careful use and rinsing of the cuvette with milliQ water consistently to ensure no contamination led to error within the results. After quite some practice with one person on the computer, one measuring into the cuvette and placing into the machine, and the final person ordering samples and passing them to the measurer, time to measure 45 samples was as short as one hour.

Figure 14: UV Vis equipment: milliQ water, KimWipes, waste beaker and standards following calibration and measurement.

Results and Discussion

The following symbols will be used throughout this section.

Table 1: Symbol Definitions.

C_A	Concentration of PEDOT
C_B	Concentration of PANI
C_Z	Concentration of ZnO
C_M	Concentration of MB

I. Adsorption Kinetics

To better understand the photocatalytic behavior of the three catalysts, the adsorption kinetics of the simulated organic pollutant (methylene blue dye) in an aqueous solution of PEDOT, PANI and ZnO have been studied through timed studies carried out under dark conditions. Adsorption kinetics are suspected to be influenced by structure, surface charge, and available 'sites' on the surface of catalyst particles. In this section the adsorption kinetics of MB in PEDOT solution will be explored and curve-fitted, which will then be compared with adsorption results from PANI and ZnO.

A. Chemical Structures:

The chemical structures of both methylene blue dye and catalysts are seen below. Both polymers have a similar ring-like structure to the organic MB dye, thus are hypothesised to have high affinity for each other. ZnO lacks these similarities and therefore is not expected to adsorb the dye as effectively as the two polymers.

MB:

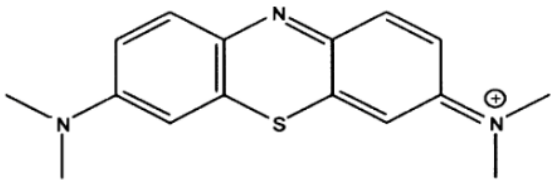

Figure 15: Chemical Structure of Methylene Blue from Hameed, Din and Ahmad, (2007) [35]

PEDOT:

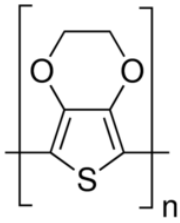

Figure 16: Chemical structure of PEDOT from Sigma Aldrich (2018)[36].

PANI:

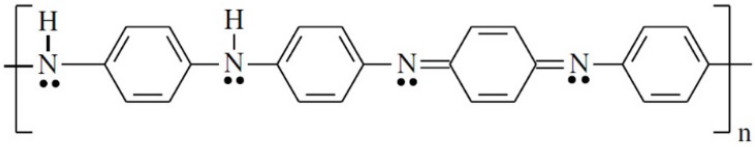

Figure 17: Chemical Structure of PANI from Mazzeu et al. (2017) [37]

ZnO

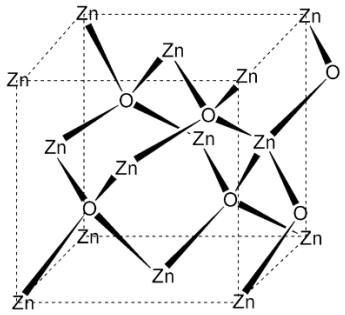

Figure 18: Chemical Structure of ZnO from ACS (2018) [38].

B. PEDOT Adsorption Study Curve-Fitting

1. First-Order Kinetics

The following graph presents results from am adsorption study, where a 32.6mgL^{-1} aqueous MB solution was stirred under dark conditions with 1gL^{-1} of sorbet, in this case PEDOT. Figure 19 shows the change in concentration of MB over time, dropping to a final concentration of 18.2mgL^{-1} at 240 minutes.

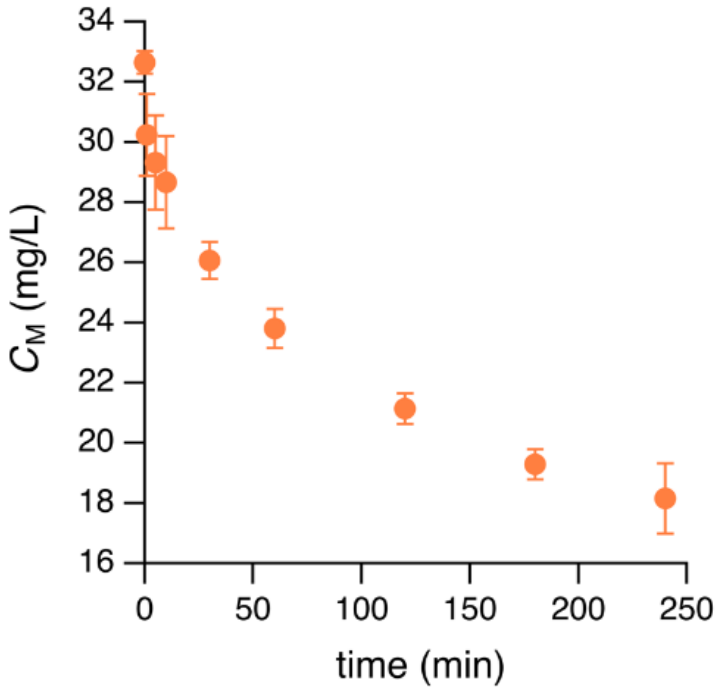

Figure 19: Kinetics of adsorption for methylene blue (initial concentration Cm0 = 32.6 mgL^{-1}) onto PEDOT (1 gL^{-1}) in an aqueous solution in the dark. Error bars signify the standard deviation of triplicate measurements.

We first assume first-order kinetics and explore the appropriateness of fit. First order kinetics would obey the law seen in Equation 1 below. The concentration dependence on time is then given by Equation 2.

Equation 1: First-Order Kinetics

$$\frac{dC_m}{dt} = -kC_m$$

Equation 2: Concentration Dependence for First-Order Kinetics

$$C_M = C_{M0}e^{-kt}$$

A straight line dependence is expected between $\ln \frac{C_{m0}}{C_m}$ and t. We plot the first order relationship as seen in the following graph, and check for a clear linear relationship in the inset plot.

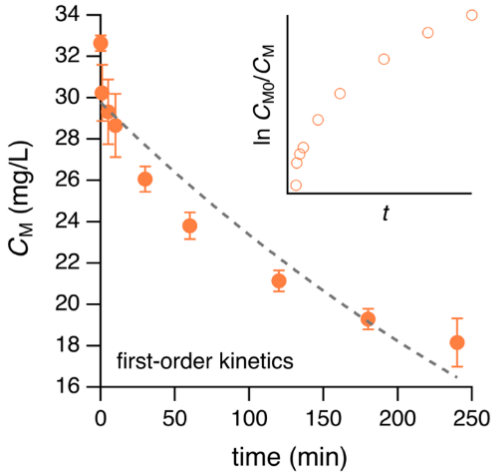

Figure 20: Adsorption data are fitted by the first-order kinetics expression in Equation 1 with C_{M0} and k as adjustable parameters, listed in Table 2. This inset plots the linearized form of Table 2, clearly showing the departure of the data from first-order kinetics.

The data are clearly not fitted by first-order kinetics, suggesting that the mechanism of adsorption depends both on the concentration of MB and on the concentration of available 'sites' on PEDOT.

For the following analysis, we therefore consider the simplest cases of pseudo first order, pseudo second order and simplified Crank adsorption kinetics. Simplified Crank adsorption is also known as power-law kinetics, or the Bangham model.

We replot the data in terms Q mg g^{-1}, the mass of adsorbate (MB) per mass of sorbent (PEDOT), noting that $Q = (C_{M0} - C_M)\, C_{PE}^{-1}$. The hypothetical maximum amount of adsorbate is given by Q_{max} and the rate constant of adsorption is given by k_{ad}.

2. Pseudo First-Order Kinetics

Pseudo first-order kinetics obey the relationship seen in Equation 3 below.

Equation 3: Pseudo First-Order Kinetics

$$Q = Q_{max}[1 - \exp(-k_{ad}t)]$$

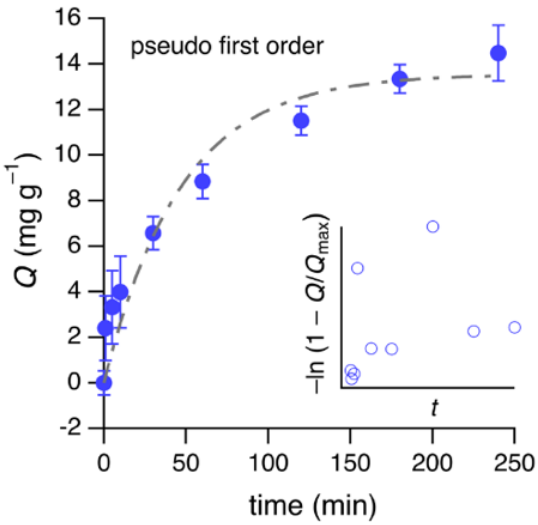

Figure 21: Adsorption data are fitted by pseudo first-order kinetics, following the relationship outlined in Equation 3.

The inset plot above clearly shows that pseudo first-order kinetics are a poor fit for the data. Pseudo Second order are considered next in the curve-fitting process.

3. Pseudo Second-Order Kinetics

Pseudo second-order kinetics obey the relationship seen in Equation 4 below.

Equation 4: Pseudo Second-Order Kinetics

$$Q = \frac{k_{ad} Q_{max}^2 t}{1 + k_{ad} Q_{max} t}$$

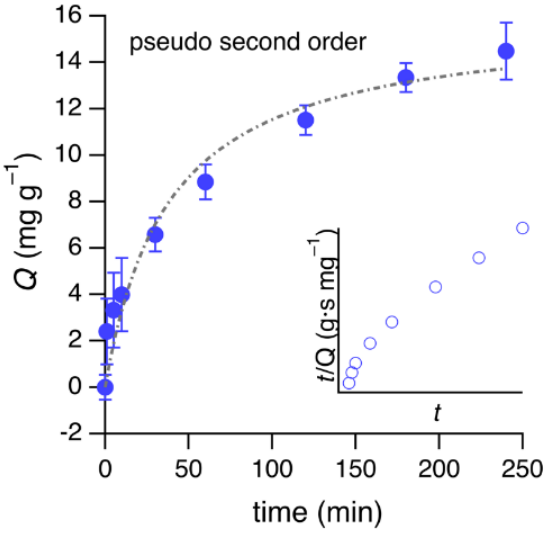

Figure 22: Adsorption data fitted by pseudo second-order kinetics following relationship in Equation 4..

The inset shows that pseudo second-order kinetic are a better fit than the previous relationships explored, however the relationship between $\ln \frac{C_{m0}}{C_m}$ and t still deviates from the expected linear relationship. We expect that this is not the right fit for the data, and continue on to fit the final Bangham power-law fit for the data.

4. Bangham Power-Law Fit

The equation for simplified Crank kinetics is essentially a Bangham power-law fit in which the exponent, n = ½. For fitting purposes, we allow both k and n to be adjustable parameters.

Equation 5: Bangham Power-Law fit

$$Q = kt^n$$

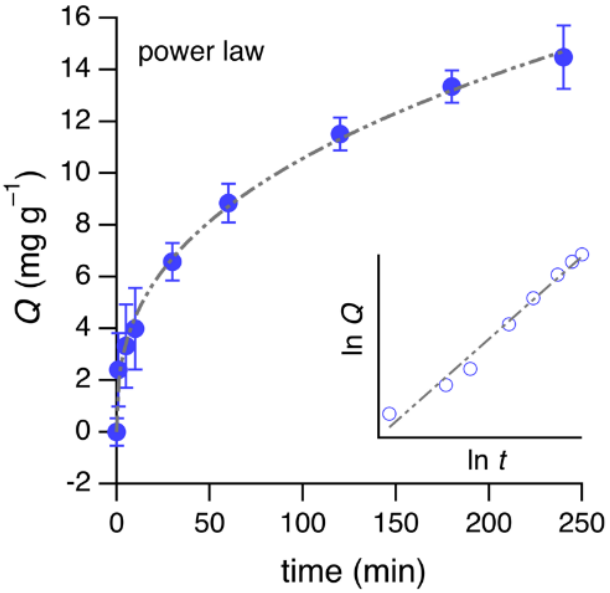

Figure 23: Adsorption data fitted by Bangham power-law fit, as seen in Equation 5 above,

The inset plot in the above figure clearly shows a linear relationship between $\ln\frac{C_{m0}}{C_m}$ and t, indicating that a Bangham power-law model is a good fit for the adsorption relationship of MB onto PEDOT.

Table 2 below shows a summary of the fitting parameters for the different fitting models. Chi-squared values were calculated from a Levenberg-Marquardt fitting algorithm and represent goodness of fit. The chi-squared value for the Bangham model is 0.648, further reinforcing the assumption made from observing the inset plot in Figure 23.

Table 2: Summary of explored kinetic relationships and fitting parameters.

Bangham		First-order		Pseudo first order		Pseudo second order	
k	1.86	C_{M0}	29.8	Q_{max}	13.6	Q_{max}	15.9
n	0.377	k	0.002	k_{ad}	0.021	k_{ad}	0.002
χ^2	0.648	χ^2	18.6	χ^2	13.1	χ^2	8.54

C. Power-Law Fit: Catalyst Comparison.

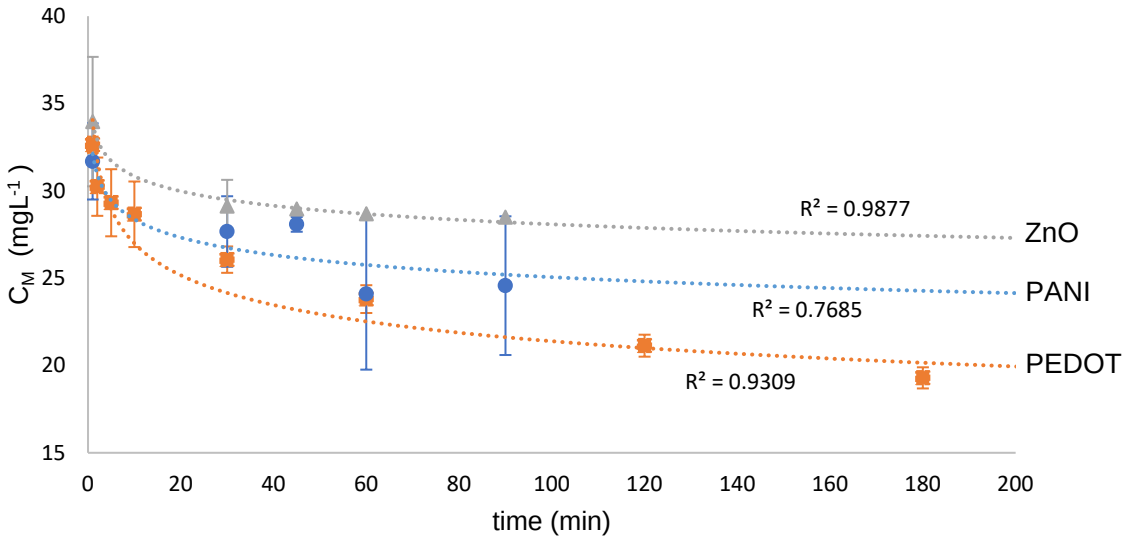

Figure 24: Comparing power-law adsorption kinetics for ▲ ZnO, ● PANI and ■ PEDOT with consistent preliminary concentration and experimental conditions. Error bars signify the standard deviation of triplicate measurements.

Figure 24 compares the previously fitted adsorption curve of MB onto PEDOT with MB onto ZnO and PANI. We fit a Bangham model power-law relationship for each sorbent, and include corresponding R-squared values. The R-squared values indicate the power-law adsorption relationship is a good fit for the additional sorbent data sets, with high ZnO and PANI R-squared values of 0.987 and 0.769 respectively. PEDOT has an R-squared value of 0.931, and has significantly higher overall adsorption efficiency than both PANI and ZnO.

The structural similarities of PEDOT and PANI seen in Section A, Figure 16 and Figure 17 respectively, suggest that adsorption of MB may follow a similar kinetic relationship for both polymers. The slightly lower R-squared value of the PANI data, however, suggests that the power-law is not as good a fit for the PANI data as it is for PEDOT. This deviation from expected behavior may be because PANI data presents with significantly larger standard deviation than the other data sets, as seen through the large error bars on the plot above. Error in the PANI data may have been due to human error, or could be due to PANI performing less efficiently as a sorbent, leading to a more randomised adsorption / desorption equilibrium behavior and thus larger variation in the results. PANI was much less successful overall as both a sorbent and photocatalyst, thus it was not analysed in the same detail in this research and presents a space for further research.

II. Photocatalysis

A. UVA Exposure

The following graph presents averages of MB dye only controls from each photocatalysis experiment. These confirm that UVA light alone cannot significantly degrade MB dye, and thus any subsequent degradation observed is due to the addition of the catalyst and the effect of either adsorption or photocatalytic processes or a combination of the two.

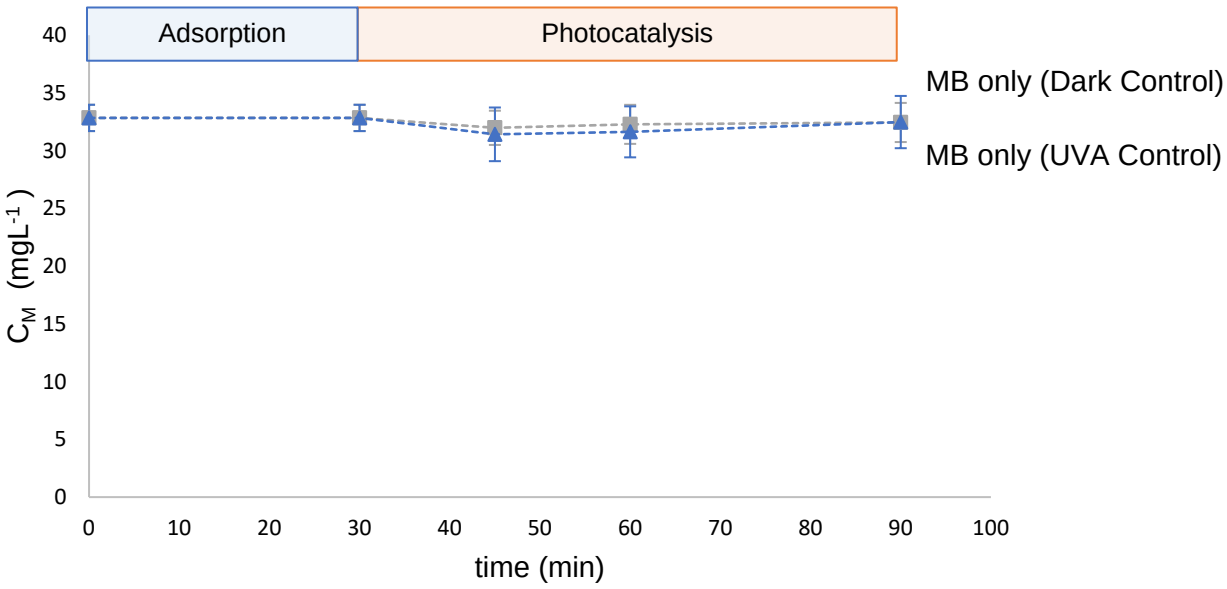

Figure 25: ▲ UV and ■ Dark control averages for all 3 catalysts (PANI, PEDOT and ZnO). Error bars signify the standard deviation of triplicate measurements. 'Adsorption' and 'Photocatalysis' labels display the experimental method of stirring 30 min under dark conditions prior to UVA light exposure.

Graphs in the following three sections show the degradation of MB dye with each photocatalyst: PEDOT, PANI and ZnO. Dark degradation data have been included on the graphs to show the effect of UVA light on the performance of the catalyst, and thus clearly display degradation rate due to photocatalysis. As explored in the previous section, degradation in dark samples is due to adsorption only. It is hypothesised that dye degradation under UV irradiation occurs via a synergistic combination of both adsorption and photocatalysis.

1. MB / PEDOT

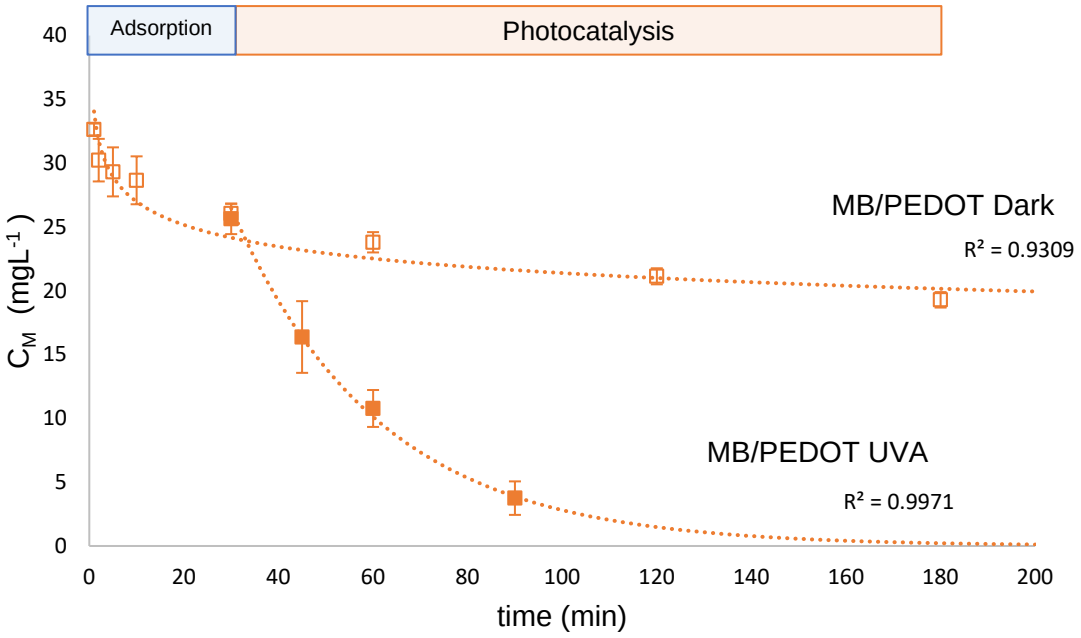

Figure 26: MB/PEDOT in ■ UVA and □ Dark conditions. All data are averages with error bars signifying standard deviation of triplicate measurements. 'Adsorption' and 'Photocatalysis' labels display the experimental method of stirring 30 min under dark conditions prior to UVA light exposure for the MB/PEDOT UVA sample. A power-law fit has been applied to the MB/PEDOT Dark sample as per the analysis in Section I.B: PEDOT Adsorption Study Curve-Fitting. The high R^2 value confirms this is a good fit for the adsorption data. MB/PEDOT UVA data has been fitted with an exponential trend, achieving a good fit represented in the high R^2 value of 0.9971.

The PEDOT data shows degradation due to both adsorption and photocatalysis, shown through a clear fall in concentration with both dark and UVA exposed samples over time. The adsorption occurs as expected, following the power-law trend. The MB/PEDOT UVA data shows clear evidence of a photocatalytic effect, closely following an exponential trend. The exponential trend is expected as photocatalysis takes some time to begin, requiring the creation of radical species to occur prior to degradation and with rate increasing with time.

Overall, there is 45% degradation of the MB/PEDOT dark sample, with dye concentration dropping from 32.9mgL^{-1} at time zero to 18.0mgL^{-1} at 180 minutes. At 90 minutes for the UVA sample, comprising of 30 minutes adsorption and 60 minutes UVA exposure, dye concentration has dropped to 3.75mgL^{-1}. This is a degradation of 88%. This degradation is double the degradation of the dye only sample in only half the time, resulting in a four-fold effect of UVA light exposure on the degradation of MB dye.

2. MB / PANI

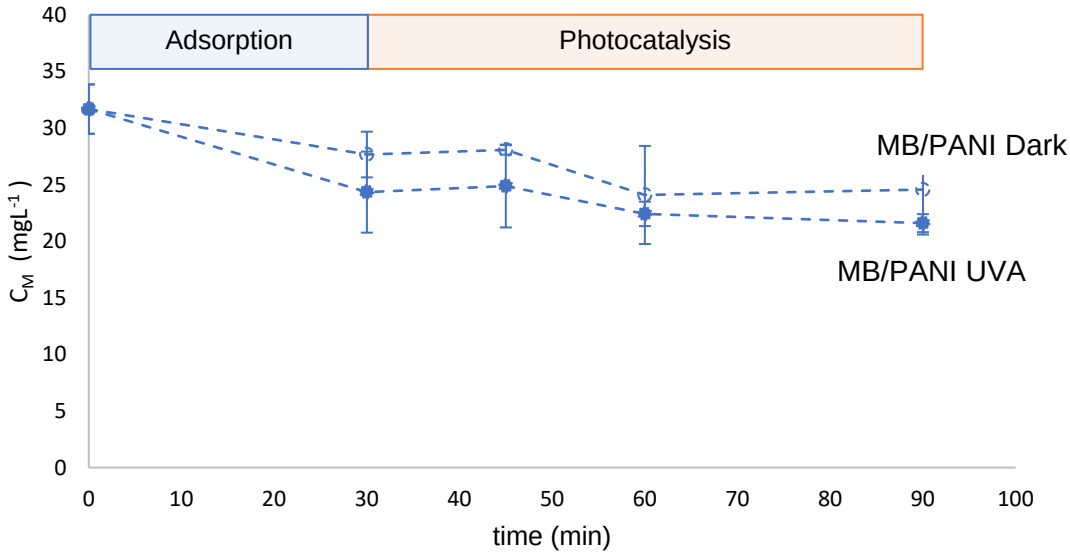

Figure 27: MB/PANI in ● UVA and ○ Dark conditions. All data are averages with error bars signifying standard deviation of triplicate measurements. 'Adsorption' and 'Photocatalysis' labels display the experimental method of stirring 30 min under dark conditions prior to UVA light exposure for the MB/PANI UVA sample. Due to the poor adsorption and photocatalytic performance of PANI, no fitting curves have been suggested.

The PANI data appears to show only a small difference between the degradation of dye through photocatalysis (UVA exposure) as compared with only adsorption (Dark sample). Furthermore, the overlap of error bars suggest the apparent increase in degradation through photocatalysis is statistically insignificant.

From this data we can conclude that if any, there is only a small amount of photocatalysis occurring with synthesised PANI powder. This could be in part due to the poor adsorption ability of PANI. As photocatalysis may be assisted by the adsorption of dye onto the surface of the polymer, a poor sorbent may also be a poor photocatalyst. Alternatively, the fundamental properties of PANI such as band gap and conductivity may be leading to poor performance, particularly the high limiting wavelength of 828nm, calculated in Section II.B.2. Following PANI's underwhelming performance, this research proceeded to focus on the higher performing polymer, PEDOT.

3. MB / ZnO

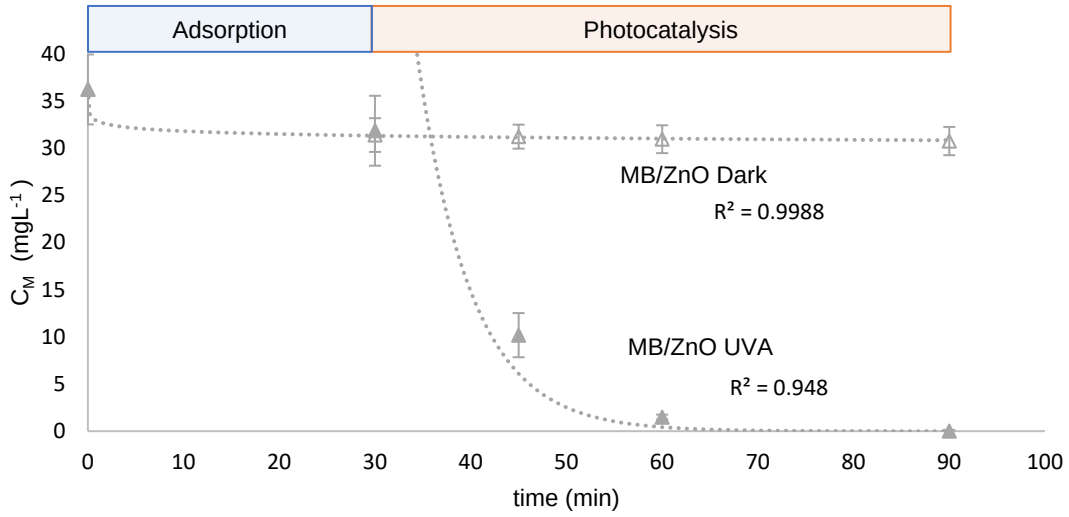

Figure 28: MB/ZnO in ▲ UVA and △ dark conditions. All data are averages with error bars signifying standard deviation of triplicate measurements. 'Adsorption' and 'Photocatalysis' labels display the experimental method of stirring 30 min under dark conditions prior to UVA light exposure for the MB/ZnO UVA sample. A power-law fit has been fitted to the MB/ZnO Dark curve, with a high R^2 value of 0.9988 suggesting this is a good fit for the data. The MB/ZnO UVA curve has been normalised to make the 90 minute value equal to 0.001mgL^{-1} (simulating zero and allowing the exponential fit), as raw UV-Vis data resulted in negative concentrations. An exponential curve has been then fitted to the data to allow comparison with PEDOT exponential curve-fitted results.

For ZnO, UVA conditions show much higher degradation levels than under dark conditions. This is unsurprising given the high performance of ZnO when exposed to UV light sources. ZnO has the largest band gap of all catalysts explored in this study, and it has therefore the shortest limiting wavelength, precluding the ability to perform visible light induced photocatalysis. UVA light, however, is well within the wavelength of light that can excite ZnO.

We fit an exponential curve to the MB/ZnO UVA data to examine the photocatalytic behavior of ZnO and allow comparison of results with the PEDOT exponential fit relationship. The resultant R-squared value of 0.948 indicates this is a good fit for the data, however on closer inspection it appears the exponential fit overestimates the x-axis values for early stages of photocatalysis. This may be due to the poor adsorption ability of ZnO, as the dye molecules are not adsorbed onto the surface of the nanoparticles and they are therefore not in close proximity to the radical species as they are formed. After an initial time period has passed, the superior photoactive properties of ZnO lead to the creation of many radical species within solution, and degradation occurs rapidly. PEDOT does not present this same delay, instead presenting rapid-onset photocatalysis due to the adsorption of dye molecules onto its' surface.

B. PEDOT Studies

Due to the high performance of PEDOT under UVA exposure the following sections explore this catalyst in further detail, particularly the effect of sorbent concentration, light exposure and pH of solution on catalyst behavior.

1. Effect of sorbent concentration.

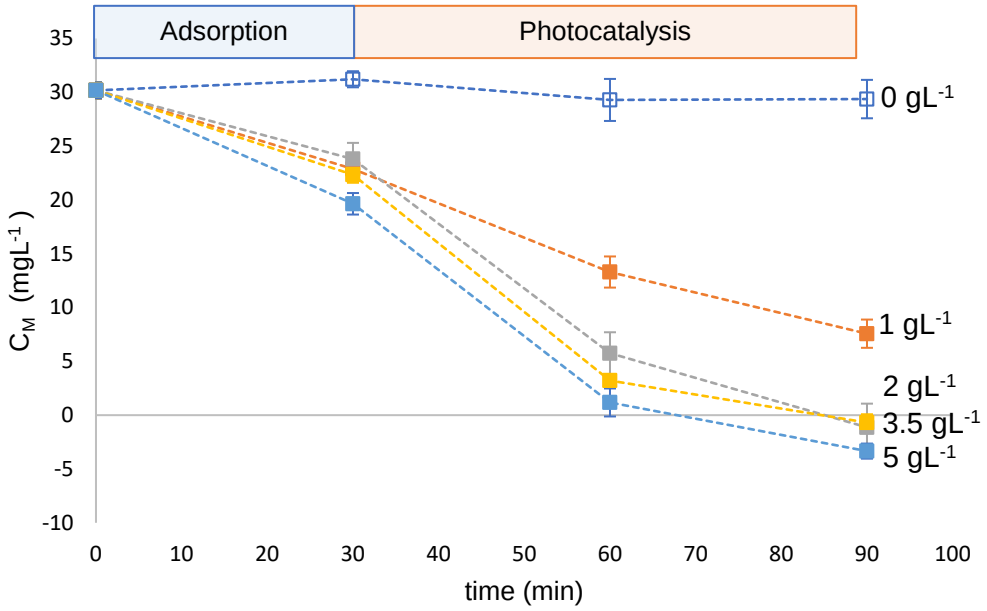

Figure 29: Change in photocatalytic effect through change in concentration of PEDOT added to solution. 0gL^{-1}; 1gL^{-1}; 2gL^{-1}; 3.5gL^{-1}; and 5gL^{-1}. All data are averages with error bars signifying standard deviation of triplicate measurements. 'Adsorption' and 'Photocatalysis' labels display the experimental method of stirring 30 min under dark conditions prior to UVA light exposure for each MB/PEDOT sample.

From this graph, the relationship between concentration of PEDOT and photocatalytic degradation is clear. At the standard amount of 1gL^{-1}, we see 78% degradation after one hour of exposure to UVA light. Doubling the concentration under the same time and light conditions to 2gL^{-1} results in 100% degradation.

At 30 minutes of UVA exposure, the 5gL^{-1} sample of PEDOT in solution has degraded to 1.2mgL^{-1}, a 96% drop in MB concentration. This higher degradation rate is due to a higher adsorption rate of the dye onto the surface of the polymer. As there are more polymer particles, the surface area increases, leading to more active 'sites' on the surface of the polymer for the dye to adsorb onto.

From the plot above we can see similar slopes for the photocatalysis sections of the curves for concentrations above $2gL^{-1}$. This suggests that there is a limit above $2gL^{-1}$ where an increase in sorbent concentration leads to a linear increase in photocatalysis. Higher performance is therefore due to the increased adsorption rate, rather than an increase in photocatalysis rate. Conversely, below this level of $2gL^{-1}$ it appears that an increase in sorbent concentration has a larger and non-linear effect on photocatalysis rate. This supports the hypothesis that it is the interaction between adsorption and free radical production processes that ultimately lead to photocatalysis and dye degradation with PEDOT catalyst.

2. Effect of light on PEDOT Degradation

The (energy) efficiency of a semiconductor depends upon its band gap; a larger band-gap material requires more energy to excite electrons into the conduction band.

$$E_g = h\nu_g = h\frac{c}{\lambda_g}$$

E_g is the band gap, usually reported in eV
h is the Planck constant, 4.14×10^{-15} eV·s
ν_g is the frequency associated with the band gap
c is the speed of light, 3×10^8 m/s
λ_g is the wavelength associated with the band gap

Table 3: Band gap and calculated limiting wavelength for the semiconductors used in this study.

	E_g (eV)	λ_g (nm)
ZnO	3.3[1]	376
PEDOT	1.4 – 2.5[2]	496
PANI	1.5[3]	828

Whilst conventional photocatalysts, like ZnO, exhibit an extremely high efficiency under UV irradiation, they are inefficient under visible light due to the wide band gap. Towards applications for water purification in the developing world, the addition of a low–band gap material, like PEDOT, enables the photocatalyst to harness a greater portion of the natural solar spectrum.

[1] V. Srikant and D.R. Clarke. *Journal of Applied Physics*. **1998**, 83, pp. 5447.
[2] L. Groenendaal *et al. Advanced Materials.* **2000**, 12, pp. 488.
[3] O. Kwon and M.L. McKee *Journal of Physical Chemistry*. **2000**, 104, pp. 1686.

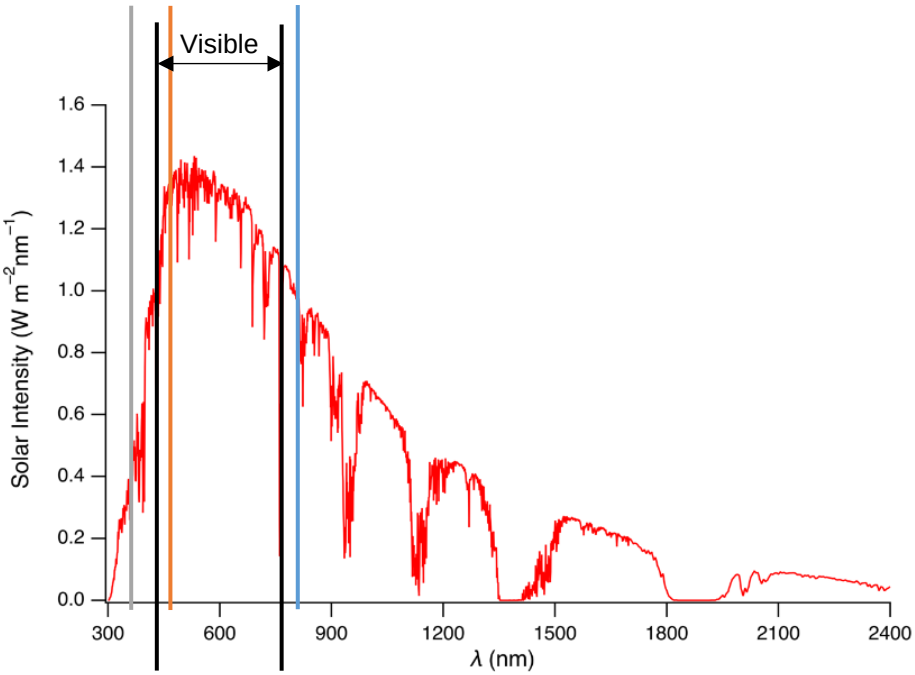

Figure 30: Solar spectrum from National Renewable Energy Laboratory, ASTM G173-03 Reference Spectra Derived from Simple Model of the Atmospheric Radiative Transfer of Sunshine SMARTS v. 2.9.2. | is the limiting wavelength of PANI at 828nm, | is the limiting wavelength of PEDOT at 496nm, and | is the limiting wavelength of ZnO at 376nm

The long limiting wavelength of PANI, at 828nm and highlighted past the visible section of the graph above, indicates it has potential to be used as a visible light activated photocatalyst. PEDOT lies just past the UV range at 496nm, also providing promise to be effective in this range. To investigate this, a study of polymer performance when exposed to different light sources has been completed.

The following graph shows the performance of a 1gL^{-1} aqueous solution of PEDOT degrading MB dye (C_{M0} = 32mgL^{-1}) under different light exposure conditions for 30 minutes, following a 30 minute adsorption period.

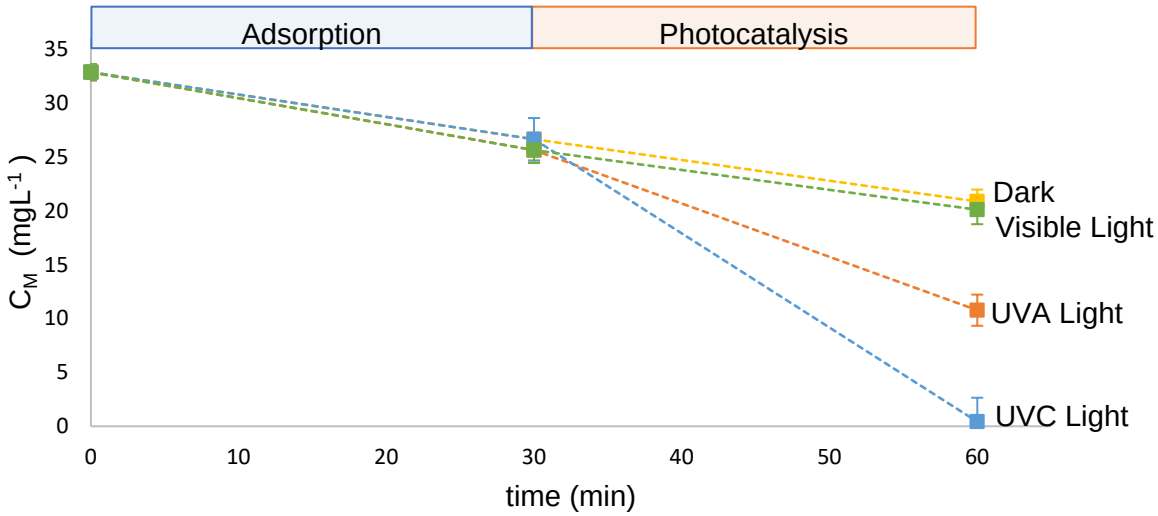

Figure 31: Effect of light source on the photocatalysis of PEDOT and degradation of MB dye. Light sources include Dark, Visible, UVA and UVC. All data are averages with error bars signifying standard deviation of triplicate measurements. 'Adsorption' and 'Photocatalysis' labels display the experimental method of stirring 30 min under dark conditions prior to light exposure.

While visible light results do not present the anticipated high performance, UVC light exposure presents promising results for PEDOT powder. UVC light delivers more energy than UVA due to the shorter wavelength, and UVC light sources are also the predominant light source used in wastewater treatment plants. Exposure time may be a factor for poor visible light performance, explored briefly in the Section 0.

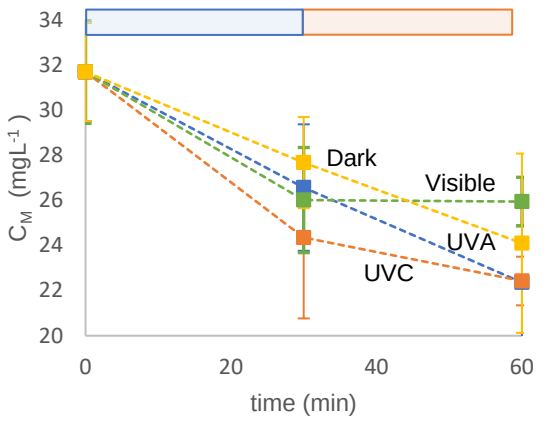

Figure 32: Effect of light source on the photocatalysis of PANI and degradation of MB dye. Light sources include Dark, Visible, UVA and UVC. All data are averages with error bars signifying standard deviation of triplicate measurements. 'Adsorption' and 'Photocatalysis' labels display the experimental method of stirring 30 min under dark conditions prior to light exposure.

Despite initial suggestions that the small band gap would present superior photocatalysis in the visible range, this was not seen in the results. More research is required to understand this unexpected behaviour.

It is possible that considering dosage would affect the conclusions from these results, as the shorter wavelength and larger irradiance values of UVC light as compared to UVA and visible light suggest more power is required to induce photocatalysis.

3. Effect of pH on catalyst activity

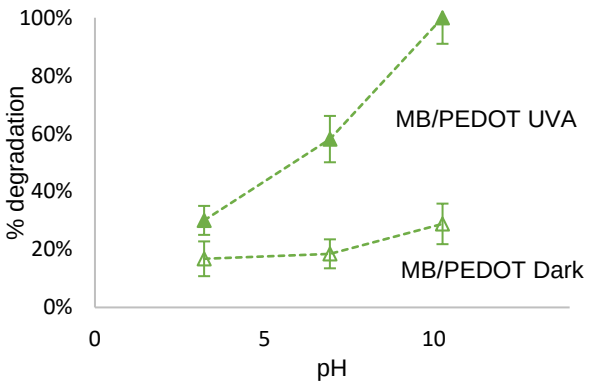

Figure 33: Effect of pH on PEDOT % degradation, where ▲ is MB/PEDOT UV and △ is MB/PEDOT Dark for different pH values of 3.22, 6.93 and 10.22 seen on x axis. MB/PEDOT sample in pH 10.22 solution reaches 100% degradation in 60 minutes UVA exposure. Error bars have been estimated from similar experiments with PEDOT during this study.

Figure 33 shows the effect of pH on PEDOT performance. It can be clearly seen that with UVA exposure, photocatalysis is favoured under basic conditions. This could be due to the increase in hydroxyl species present in basic solutions. This suggests that hydroxyl radicals may play a large role in MB degradation via photocatalysis. This is a hypothesis that will be further tested in the following mechanistic studies section.

4. Mechanism Studies

In order to better understand the behavior of PEDOT based photocatalysis, the mechanism of reaction has been explored via the addition of radical scavengers within solution.

a) Hydroxyl Radicals.

To test for hydroxyl radicals, 0.1M *tert*-Butanol was added to standard MB dye and PEDOT solutions for the UV experiment. *Tert*-Butanol (TBu) is a tertiary alcohol that is very easily oxidized by hydroxyl radicals and acts as a scavenger, removing OH radicals from solution as they are formed and preventing dye degradation. The results below suggests that OH radicals do play a role in the degradation of MB dye with PEDOT.

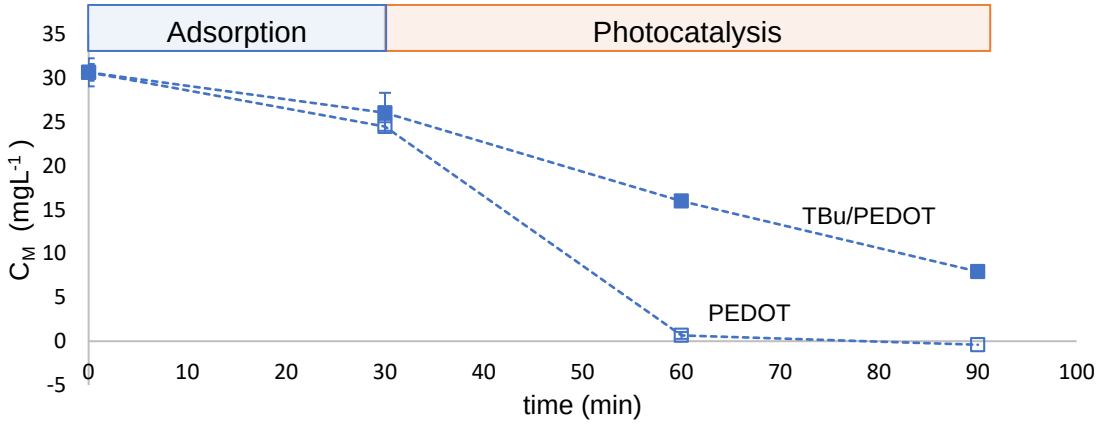

Figure 34: Hydroxyl Radical analysis through addition of radical scavenger tert-Butanol. ■ is TBu/PEDOT sample with radical scavenger, while □ is PEDOT sample in MB with no addition of tertiary butanol All data are averages with error bars signifying standard deviation of triplicate measurements. 'Adsorption' and 'Photocatalysis' labels display the experimental method of stirring 30 min under dark conditions prior to UVA light exposure. Radical scavenged sample shows 74% degradation after 90 minutes, whereas PEDOT only sample presents 100% degradation of MB dye at 90 minutes.

b) Super Oxide Radicals

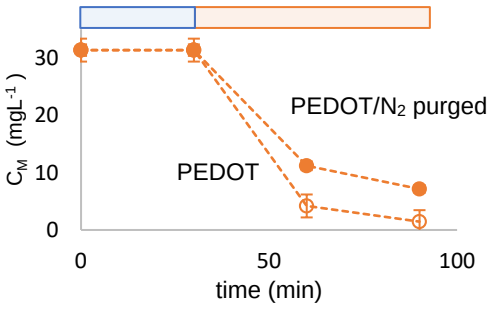

Figure 35: Superoxide radical analysis through N2 purging. Error bars have been estimated via similar PEDOT experiments undertaken during this study. ● is PEDOT in N_2 purged solution to remove O_2 species and hinder the creation of superoxide radicals. ○ is the standard MB/PEDOT experiment with 1gL^{-1}PEDOT in aqueous solution of MB dye (C_M = 31.36mgL^{-1}). Blue bar represents adsorption period of 30 minutes, and orange bar represents photocatalysis with UVA exposure for 60 minutes.

Purging with nitrogen gas removes O_2 gas from solution. By doing this, the number of superoxide radicals that can be created is lower as there are no available Oxygen molecules. Only a small loss in performance is seen. It cannot be confirmed if this is due to superoxide radicals not playing a large role in photocatalysis, or, if experimental constraints of only a short purging time has led to Oxygen species remaining in solution.

III. Composites

While PEDOT in particular shows superior photocatalytic ability at relatively high concentrations, as the following graph presents, ZnO is a successful photocatalyst even at low concentrations. Polymer/ZnO composites have promise to increase performance both of the polymer under UV exposure, and potentially also of ZnO in the visible light spectrum. In the following sections, mixtures of polymer and ZnO were examined for their performance during adsorption and subsequent exposure to UVA light.

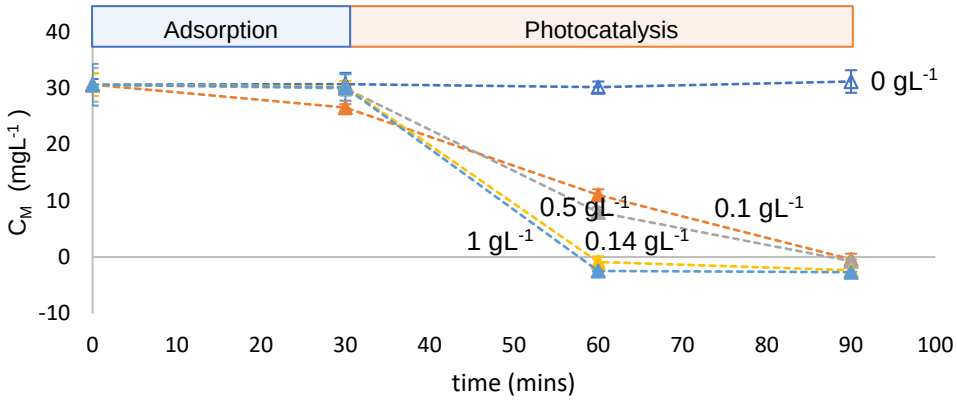

Figure 36: Photocatalysis with ZnO nanoparticles at different concentrations. Error bars have been estimated from similar ZnO results during this research. △ is 0 gL^{-1}ZnO nanoparticles in MB solution, ▲ is 0.1 gL^{-1}, ▲ is 0.14 gL^{-1}, ▲ is 3.5 gL^{-1}, and ▲ is 1 gL^{-1} sample.

The goal of this section is to determine whether there are any interactive processes occurring, either positive or negative, between the polymer and ZnO. Of particular note is to be careful if there is any decrease in ZnO performance with the addition of polymer.

A. PEDOT + ZnO

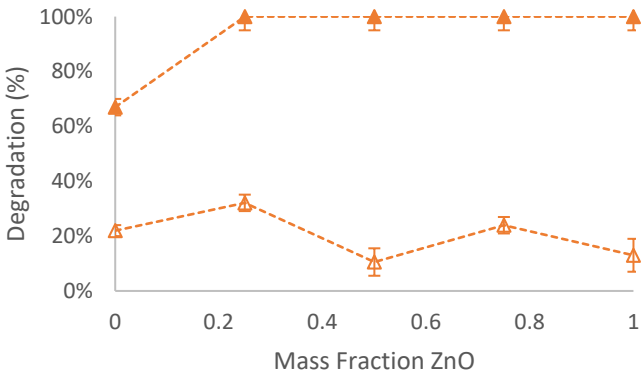

Figure 37: Mixture of PEDOT / ZnO in MB solution. △ represents percent degradation after 30 minutes of adsorption, while ▲ represents percent degradation following 30 minutes of UVA exposure. Error bars have been estimated from previous experiments completed in this research. Total catalyst mixture concentration (PEDOT + ZnO) in MB solution is 1 gL^{-1}.

Figure 37 shows the performance of a ZnO/PEDOT mixture under UVA light. Interestingly, after 30 minutes of adsorption there is a similar amount of degradation regardless of mass fraction ZnO, which contrasts previous results suggesting PEDOT should increase degradation via adsorption through its superior sorbent properties. If we look closer at the data, however, we see that the maximum concentration is in the sample with mass fraction ZnO at 0, which is, in total, 1gL^{-1} PEDOT. As this is still at the lower limit of PEDOT concentration required for adsorption as studied in Section II.B.1 Effect of Sorbent Concentration, we can predict that higher total levels of PEDOT/ZnO mixture in solution may present a trend that is closer to expected. Further analysis and experimentation is necessary.

B. PANI + ZnO

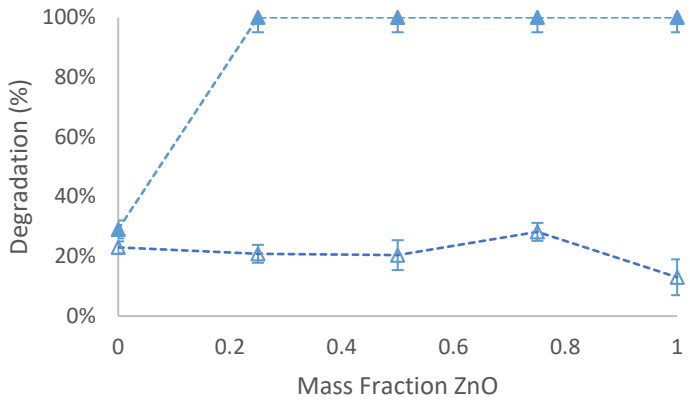

Figure 38: Mixture of PANI / ZnO in MB solution. △ represents percent degradation after 30 minutes of adsorption, while ▲ represents percent degradation after 30 minutes of UVA exposure. Error bars have been estimated from previous experiments completed in this research. Total catalyst mixture concentration (PANI + ZnO) in MB solution is 1 gL^{-1}.

As seen in Figure 38 above, while the poor performance of PANI was expected in the pure PANI sample, at ZnO mass fraction zero, it is promising to note that PANI does not hinder in any way the photocatalytic performance of ZnO in any way. This, perhaps redeeming quality of PANI suggests a composite of PANI/ZnO could be successful under UVA light and potentially under visible light also. Again, further experimentation is required, particularly in the case of a PANI based composite and investigating the ability of these to perform in both the UV and visible light spectrum.

As can be seen in the appendices, attempts to make both composites proved unsuccessful, confirmed through the XRD graphs that show no clear ZnO peaks. Further research is required to attempt to make such composites successfully.

Future Work: Applications and Limitations

When considering the applications and future development of this technology, there are a number of important factors and limitations to take into account. Incorporating the following points into future design processes could lead to the creation of a technology that is one step closer to answering issues around global water scarcity and emerging contaminants.

- In this study methylene blue has been used to model organic pollutants in wastewater. Further study will need to take place into whether MB is in fact an appropriate model and whether PEDOT is as effective at degrading trace amounts of either pharmaceuticals or pathogens in real wastewater as it is at degrading large quantities of MB.

- If the application focus was for treatment in more developed countries, such as New Zealand, to target emerging contaminants, reactor configuration would need to be continuous in order to be remain relevant.

- As PEDOT has shown success with the UVA light source, the higher energy UVC that is currently used in water treatment plants will be sufficient for the onset of photocatalysis, however residence time would need to be carefully considered.

- Industrial dyes, for example from the textile industry or other plant-based dyes following processes such as paper processing. With the rise of responsible manufacture and the desire for companies to protect ecosystems by not disposing of harmful dyes and other pollutants, there may be opportunities for further development in these spaces.

- Regarding treatment in the developing world, this is a high-risk environment that requires robust and both easily operable and maintainable technology. Whilst photocatalysis using semiconducting polymers is a technology that could be stretched into the visible light range, questions around appropriateness for developing or rural areas would need to be cautiously considered. This is certainly an application space where the question **‘can we do it?’** must be soon followed by **‘should we do it?’**

Conclusions

- Photocatalysis has been highlighted as a potential solution to complex wastewater problems including emerging contaminants and inadequate water treatment methods in the developing world, particularly due to opportunities in visible light activated photocatalysis.
- PEDOT, PANI and ZnO have been studied to explore the photocatalytic degradation of MB dye and to simulate organic contaminants in wastewater.
- Out of the two polymers, PEDOT is by far the highest performing photocatalyst, achieving 88% degradation after one hour of UVA exposure.
- Adsorption of MB dye onto PEDOT is best modelled with a power-law relationship.
- Above 2g/L of PEDOT there is a linear increase in degradation with no change in degradation rate. This indicates there is an adsorption limit below which an increase in polymer concentration has a non-linear effect on photocatalysis.
- Degradation of MB with PEDOT favours basic conditions.
- ZnO presents extremely effective photocatalysis under UV light exposure.
- PEDOT presents ‘rapid-onset’ photocatalysis, due to the high adsorption ability and the interaction between adsorption and photocatalytic properties. ZnO, although extremely efficient, has a delay in the onset of photocatalysis as there is little adsorption and time is taken for hydroxyl radicals to form.
- PANI achieves underwhelming results in every category, due to poor adsorption ability and poor free radical production. More investigation is required, particularly with synthesis routes and doping opportunities.
- Composites of polymer and ZnO are promising avenues for further research and have been proven here to show success through testing of mixtures.
- Future work suggests that there is scope for further development of this technology, particularly considering important aspects such as reactor residence time, visible light activation, material cost and process reliability.

References

[1] UNESCO-WAAP, “Water for People, Water for Life,” 2003.

[2] J. Pruss A. Kay D. Fewtrell L. Bartram, “Estimating the burden of disease,” *Environ. Health Perspect.*, vol. 110, no. 5, pp. 537–542, 2002.

[3] UNESCO-WAAP, “Nature Based Solutions for Water,” 2018.

[4] F. M. Gimelli, J. J. Bos, and B. C. Rogers, “Fostering equity and wellbeing through water: A reinterpretation of the goal of securing access,” *World Dev.*, vol. 104, pp. 1–9, 2018.

[5] Z. Burt *et al.*, “User preferences and willingness to pay for safe drinking water: Experimental evidence from rural Tanzania,” *Soc. Sci. Med.*, vol. 173, pp. 63–71, 2017.

[6] UNDP, “Sustainable Development Goals,” 2015.

[7] United Nations (UN), “Global Sustainable Development Report,” p. 134, 2016.

[8] M. Starkl, N. Brunner, and T. A. Stenström, “Why do water and sanitation systems for the poor still fail? Policy analysis in economically advanced developing countries,” *Environ. Sci. Technol.*, vol. 47, no. 12, pp. 6102–6110, 2013.

[9] M. Shatat, M. Worall, and S. Riffat, “Opportunities for solar water desalination worldwide: Review,” *Sustain. Cities Soc.*, vol. 9, pp. 67–80, 2013.

[10] P. Hutchings *et al.*, “A systematic review of success factors in the community management of rural water supplies over the past 30 years,” *Water Policy*, vol. 17, no. 5, pp. 963–983, 2015.

[11] A. Jiménez and A. Pérez-Foguet, “The relationship between technology and functionality of rural water points: Evidence from Tanzania,” *Water Sci. Technol.*, vol. 63, no. 5, pp. 948–955, 2011.

[12] C. (Environmental S. and R. L. Nokes, “An Introduction to Drinking Water Contaminants, Treatment and Management,” no. June, pp. 15–29, 2008.

[13] D. S. Lantagne, “Viability of commercially available bleach for water treatment in developing countries,” *Am. J. Public Health*, vol. 99, no. 11, pp. 1975–1978, 2009.

[14] UNESCO-WAAP, “Wastewater: The Untapped Resource,” 2017.

[15] L. Prieto-Rodriguez, S. Miralles-Cuevas, I. Oller, A. Agüera, G. L. Puma, and S. Malato, “Treatment of emerging contaminants in wastewater treatment plants (WWTP) effluents by solar photocatalysis using low TiO2concentrations,” *J. Hazard. Mater.*, vol. 211–212, pp. 131–137, 2012.

[16] N. Serpone and A. V. Emeline, “Semiconductor photocatalysis - Past, present, and future outlook,” *J. Phys. Chem. Lett.*, vol. 3, no. 5, pp. 673–677, 2012.

[17] Y. Ohko *et al.*, “17β-estradiol degradation by TiO2 photocatalysis as a means of reducing estrogenic activity,” *Environ. Sci. Technol.*, vol. 36, no. 19, pp. 4175–4181, 2002.

[18] P. Kumar, K. Hegde, S. K. Brar, M. Cledon, and A. Kermanshahi Pour, “Physico-chemical treatment for the degradation of cyanotoxins with emphasis on drinking water treatment - How far have we come?,” *J. Environ. Chem. Eng.*, vol. 6, no. 4, pp. 5369–5388, 2018.

[19] D. Kanakaraju, B. D. Glass, and M. Oelgemöller, “Advanced oxidation process-mediated removal of pharmaceuticals from water: A review,” *J. Environ. Manage.*, vol. 219, pp. 189–207, 2018.

[20] A. J. Ebele, M. Abou-Elwafa Abdallah, and S. Harrad, “Pharmaceuticals and personal care products (PPCPs) in the freshwater aquatic environment,” *Emerging Contaminants*, vol. 3, no. 1. Elsevier Ltd, pp. 1–16, 2017.

[21] S. Ghosh *et al.*, “Visible-light active conducting polymer nanostructures with superior

photocatalytic activity," *Sci. Rep.*, vol. 5, pp. 1–9, 2015.
[22] S. Dong *et al.*, "Recent developments in heterogeneous photocatalytic water treatment using visible light-responsive photocatalysts: a review," *RSC Adv.*, vol. 5, no. 19, pp. 14610–14630, 2015.
[23] K. M. Lee, C. W. Lai, K. S. Ngai, and J. C. Juan, "Recent developments of zinc oxide based photocatalyst in water treatment technology: A review," *Water Res.*, vol. 88, pp. 428–448, 2016.
[24] N. F. F. Moreira *et al.*, "Photocatalytic ozonation of urban wastewater and surface water using immobilized TiO2with LEDs: Micropollutants, antibiotic resistance genes and estrogenic activity," *Water Res.*, vol. 94, pp. 10–22, 2016.
[25] J. T. Adeleke, T. Theivasanthi, M. Thiruppathi, M. Swaminathan, T. Akomolafe, and A. B. Alabi, "Photocatalytic degradation of methylene blue by ZnO/NiFe2O4nanoparticles," *Appl. Surf. Sci.*, vol. 455, no. April, pp. 195–200, 2018.
[26] W. Wang, G. Huang, J. C. Yu, and P. K. Wong, "Advances in photocatalytic disinfection of bacteria: Development of photocatalysts and mechanisms," *J. Environ. Sci. (China)*, vol. 34, pp. 232–247, 2015.
[27] M. Wang, G. Yang, P. Jin, H. Tang, H. Wang, and Y. Chen, "Highly hydrophilic poly(vinylidene fluoride)/meso-titania hybrid mesoporous membrane for photocatalytic membrane reactor in water," *Sci. Rep.*, vol. 6, no. August 2015, pp. 1–10, 2016.
[28] B. L. Groenendaal, F. Jonas, D. Freitag, H. Pielartzik, and J. R. Reynolds, "Poly(3,4-ethylenedioxythiophene) and Its Derivatives- Past, Present, and Future.pdf," pp. 481–494, 2000.
[29] W. Shi, Q. Yao, S. Qu, H. Chen, T. Zhang, and L. Chen, "Micron-thick highly conductive PEDOT films synthesized via self-inhibited polymerization: roles of anions," *NPG Asia Mater.*, vol. 9, no. 7, p. e405, 2017.
[30] R. Saravanan, E. Sacari, F. Gracia, M. M. Khan, E. Mosquera, and V. K. Gupta, "Conducting PANI stimulated ZnO system for visible light photocatalytic degradation of coloured dyes," *J. Mol. Liq.*, vol. 221, pp. 1029–1033, 2016.
[31] V. Eskizeybek, F. Sari, H. Gülce, A. Gülce, and A. Avci, "Preparation of the new polyaniline/ZnO nanocomposite and its photocatalytic activity for degradation of methylene blue and malachite green dyes under UV and natural sun lights irradiations," *Appl. Catal. B Environ.*, vol. 119–120, pp. 197–206, 2012.
[32] X. Li, D. Wang, G. Cheng, Q. Luo, J. An, and Y. Wang, "Preparation of polyaniline-modified TiO2 nanoparticles and their photocatalytic activity under visible light illumination," *Appl. Catal. B Environ.*, vol. 81, no. 3–4, pp. 267–273, 2008.
[33] T. C. Mo, H. W. Wang, S. Y. Chen, and Y. C. Yeh, "Synthesis and dielectric properties of polyaniline/titanium dioxide nanocomposites," *Ceram. Int.*, vol. 34, no. 7, pp. 1767–1771, 2008.
[34] V. Gilja, K. Novaković, J. Travas-Sejdic, Z. Hrnjak-Murgić, M. K. Roković, and M. Žic, "Stability and Synergistic Effect of Polyaniline/TiO2 Photocatalysts in Degradation of Azo Dye in Wastewater," *Nanomaterials*, vol. 7, no. 12, p. 412, 2017.
[35] B. H. Hameed, A. T. M. Din, and A. L. Ahmad, "Adsorption of methylene blue onto bamboo-based activated carbon: Kinetics and equilibrium studies," *J. Hazard. Mater.*, vol. 141, no. 3, pp. 819–825, 2007.
[36] Sigma Aldrich, "Poly(3,4-ethylenedioxythiophene)," *Product Specifications*, 2018. .
[37] M. A. C. Mazzeu, L. K. Faria, A. de M. Cardoso, A. M. Gama, M. R. Baldan, and E. S. Gonçalves, "Structural and morphological characteristics of polyaniline synthesized in pilot scale," *J. Aerosp. Technol. Manag.*, vol. 9, no. 1, pp. 39–47, 2017.
[38] American Chemical Society, "Zinc Oxide," *Molecule of the Week*, 2014. .

Appendices

The following present graphs / data that was not included in the report.

Curve-fitting with more data analysis:

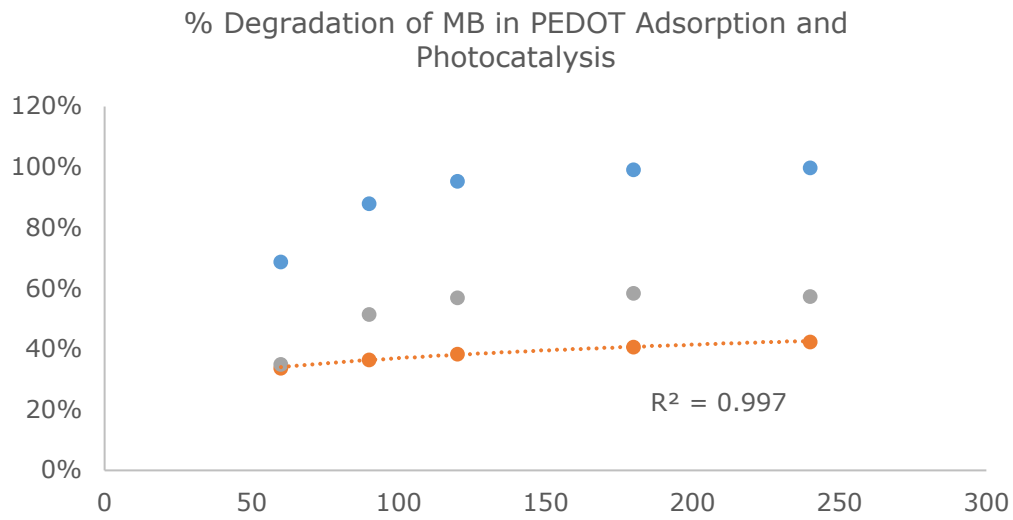

Curve-fit with adsorption power-law fit
Orange: degradation via adsorption.
Blue: observed degradation (photocatalysis and adsorption).
Grey line = blue line – orange line.
Therefore, grey may be effect of photocatalysis ONLY, is something to be further explored.

Actual ZnO data
Pre-transformation to ensure values are above zero, when 90 min point = 0.001mg/L.

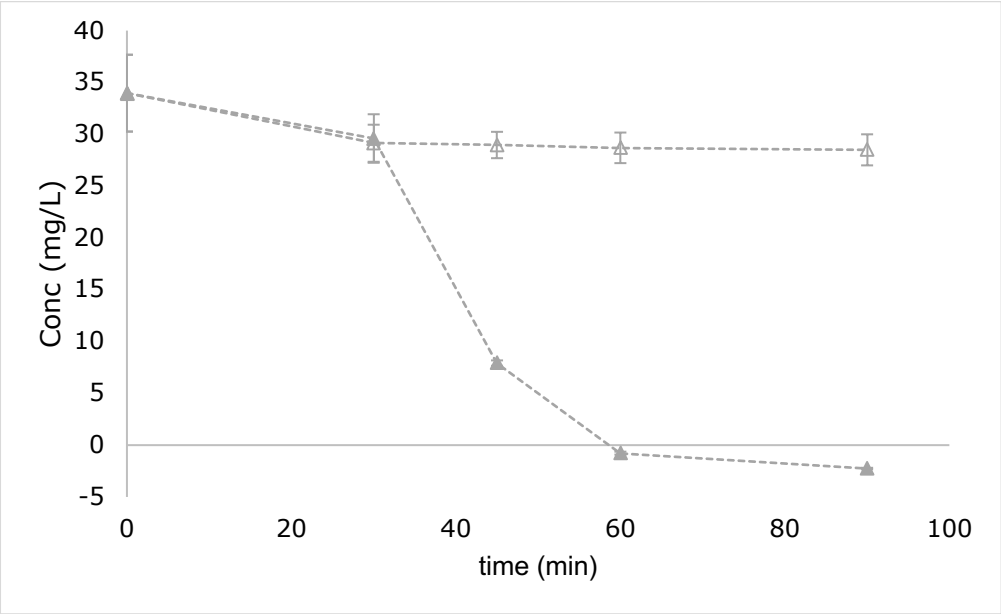

ZnO peaks XRD:

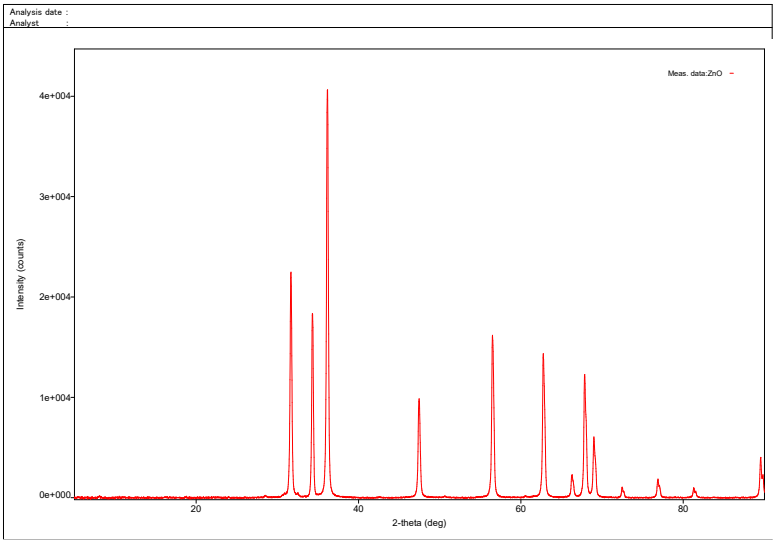

Looking of these peaks in subsequent composite attempts:

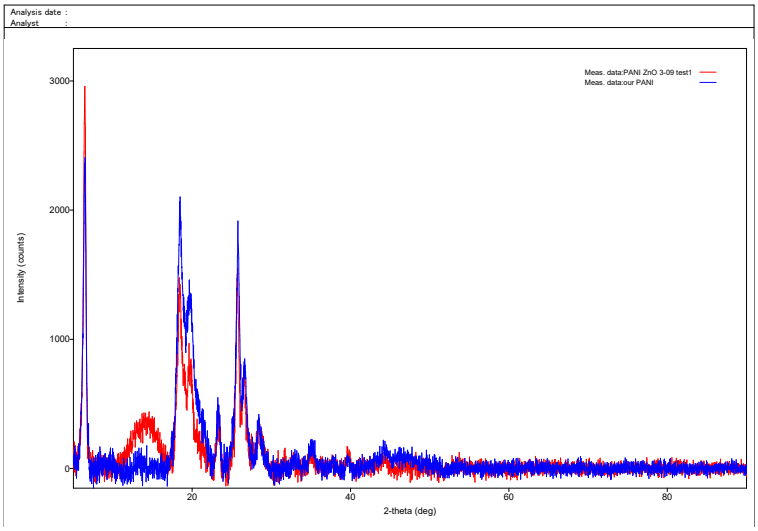

This shows PANI/ZnO compared with PANI only. As can be clearly seen, there is no difference between the two curves suggesting no presence of ZnO, particularly as the ZnO peaks are very distinct (as seen above).

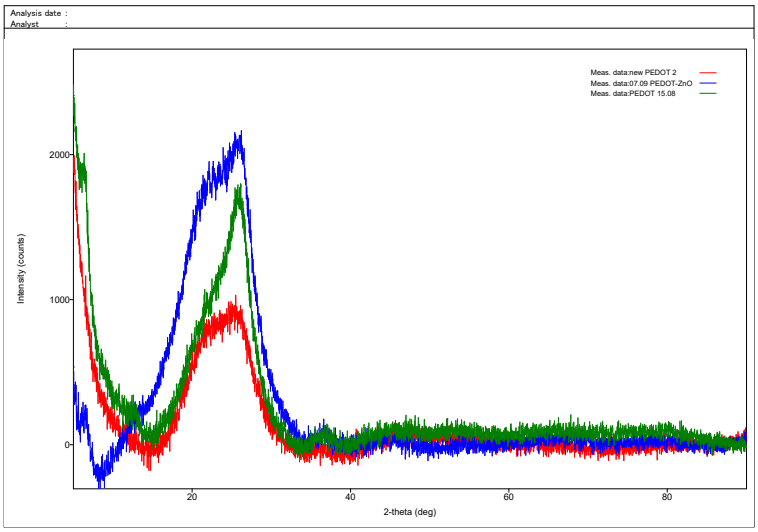

This shows three curves: two different samples of PEDOT (the red and green), and the PEDOT/ZnO composite attempt in blue. Once again, no obvious presence of ZnO

HAZOP, MSDS and Lab Sign-Off

Potential Hazards	Consequences	Safeguards
Contact with chemicals	Skin/eye irritation, burns or other health problems	Always wear protective clothing (lab coats, safety glasses, appropriate gloves and masks) when handling chemicals.
High temperatures - of glass being heated in water bath, exothermic reaction of catalyst with water.	Burns, damage to equipment.	Use correct insulation gloves when handling samples that have been heated; use metal tongs or tweezers as appropriate.
Flammable solvents used for cleaning samples (ethanol / methanol)	Fire/explosion	Clean samples away from any heat source or ignition sources. Also ensure lids of containers storing these chemicals are closed always when not in use; store solvent in the designated cabinet when not in use.
Spillage	Toxic fumes, potential fire hazard, slip / trip.	Ensure lids are closed when not in use. Ground all equipment containing material and do not place chemical where it can be easily knocked over and keep spillage away from heat.
Sharp blades/scissors in cutting samples / labels	Cuts	Use appropriate scissors for the task, when using razor blades cut away from yourself on a hard surface.
Use of vacuum pump leads to solvent to be pumped into the air.	Inhalation of solvent.	Ensure the pump does not pump for too long, or over-pump the solvent from the vessel into the surrounding air. Only use the pump at intermittent intervals and do not run pump continuously for a long period of time.
Ingestion of chemicals	Intoxication	Do not drink anything in the labs including water as many chemicals are also colourless liquids
Breakage of glass vials / containers within the lab.	Injury / harm due to cuts, injury when cleaning up off the floor.	Ensure good communication when something is broken, clean straight away with proper gloves / equipment / spill kits.
Disposal of waste materials is done poorly and causes adverse reaction.	Potential reaction of oxidising ferric chloride in waste slurry with acids if stored nearby – potential explosion.	Make sure waste containers are well labelled with details of exactly what is inside. Do not store the ferric chloride/ oxidising waste container next to one that contains acid.

SAFETY DATA SHEET

Version 5.6
Revision Date 27.09.2017
Print Date 12.10.2018

1. IDENTIFICATION OF THE SUBSTANCE/MIXTURE AND OF THE COMPANY/UNDERTAKING

1.1 Product identifiers

Product name : Aniline

Product Number : 242284
Brand : Sigma-Aldrich

1.2 Other means of identification

No data available

1.3 Relevant identified uses of the substance or mixture and uses advised against

For R&D use only. Not for pharmaceutical, household or other uses.

1.4 Details of the supplier of the safety data sheet

Company : Sigma-Aldrich New Zealand Co.
PO BOX 106-406
1030 AUCKLAND
NEW ZEALAND

Telephone : 0800 936 666

1.5 Emergency telephone number

Emergency Phone # : 0800 928 888 (NZ)
+64 9 801 0034 (Int'l CHEMTREC)

2. HAZARDS IDENTIFICATION

2.1 GHS Classification

Flammable Liquids (Category D)
Acute toxicity, Oral (Category C)
Acute toxicity, Inhalation (Category B)
Acute toxicity, Dermal (Category C)
Skin irritation (Category A)
Serious eye damage (Category A)
Skin sensitisation (Category B)
Germ cell mutagenicity (Category B)
Carcinogenicity (Category B)
Aquatic toxicity (Acute or Chronic) (Category A)

2.2 GHS Label elements, including precautionary statements

Pictogram

Signal word Danger

Hazard statement(s)
H227 Combustible liquid.
H301 Toxic if swallowed.
H311 Toxic in contact with skin.

SAFETY DATA SHEET

Version 5.5
Revision Date 17.11.2014
Print Date 18.10.2018

1. IDENTIFICATION OF THE SUBSTANCE/MIXTURE AND OF THE COMPANY/UNDERTAKING

1.1 Product identifiers

Product name : Ammonium persulfate

Product Number : 248614
Brand : Sigma-Aldrich

1.2 Other means of identification

AP
Ammonium peroxodisulfate
APS
PER
Ammonium peroxydisulfate

1.3 Relevant identified uses of the substance or mixture and uses advised against

For R&D use only. Not for pharmaceutical, household or other uses.

1.4 Details of the supplier of the safety data sheet

Company : Sigma-Aldrich New Zealand Co.
PO BOX 106-406
1030 AUCKLAND
NEW ZEALAND

Telephone : 0800 936 666

1.5 Emergency telephone number

Emergency Phone # : 0800 928 888 (NZ)
+64 9 801 0034 (Int'l CHEMTREC)

2. HAZARDS IDENTIFICATION

2.1 GHS Classification

Oxidizing liquids or solids (Category C)
Acute toxicity, Oral (Category D)
Acute toxicity, Dermal (Category D)
Respiratory sensitisation (Category A)
Skin sensitisation (Category B)
Aquatic toxicity (Acute or Chronic) (Category D)

2.2 GHS Label elements, including precautionary statements

Pictogram

Signal word Danger

Hazard statement(s)

H272	May intensify fire; oxidiser.
H302	Harmful if swallowed.
H312	Harmful in contact with skin.
H317	May cause an allergic skin reaction.
H334	May cause allergy or asthma symptoms or breathing difficulties if inhaled.
H402	Harmful to aquatic life.

SAFETY DATA SHEET

Version 5.9
Revision Date 11.06.2018
Print Date 18.10.2018

1. IDENTIFICATION OF THE SUBSTANCE/MIXTURE AND OF THE COMPANY/UNDERTAKING

1.1 Product identifiers

Product name : Diethylene glycol

Product Number : H26456
Brand : Sigma-Aldrich

1.2 Other means of identification

2,2′-Oxydiethanol
Bis(2-hydroxyethyl) ether
Diglycol
2-Hydroxyethyl ether

1.3 Relevant identified uses of the substance or mixture and uses advised against

For R&D use only. Not for pharmaceutical, household or other uses.

1.4 Details of the supplier of the safety data sheet

Company : Sigma-Aldrich New Zealand Co.
PO BOX 106-406
1030 AUCKLAND
NEW ZEALAND

Telephone : 0800 936 666

1.5 Emergency telephone number

Emergency Phone # : 0800 928 888 (NZ)
+64 9 801 0034 (Int'l CHEMTREC)

2. HAZARDS IDENTIFICATION

2.1 GHS Classification

Acute toxicity, Oral (Category D)
Skin irritation (Category B)
Eye irritation (Category A)

2.2 GHS Label elements, including precautionary statements

Pictogram

Signal word Warning

Hazard statement(s)
H302 Harmful if swallowed.
H316 Causes mild skin irritation.
H320 Causes eye irritation.

Precautionary statement(s)

Prevention
P264 Wash skin thoroughly after handling.

SAFETY DATA SHEET

according to Regulation (EC) No. 1907/2006
Version 5.1 Revision Date 10.12.2014
Print Date 18.10.2018
GENERIC EU MSDS - NO COUNTRY SPECIFIC DATA - NO OEL DATA

SECTION 1: Identification of the substance/mixture and of the company/undertaking

1.1 Product identifiers

Product name : 3,4-Ethylenedioxythiophene

Product Number : 483028
Brand : Aldrich
REACH No. : A registration number is not available for this substance as the substance or its uses are exempted from registration, the annual tonnage does not require a registration or the registration is envisaged for a later registration deadline.
CAS-No. : 126213-50-1

1.2 Relevant identified uses of the substance or mixture and uses advised against

Identified uses : Laboratory chemicals, Manufacture of substances

1.3 Details of the supplier of the safety data sheet

Company : Sigma-Aldrich New Zealand Co.
PO BOX 106-406
1030 AUCKLAND
NEW ZEALAND

Telephone : 0800 936 666

1.4 Emergency telephone number

Emergency Phone # : 0800 928 888 (NZ)
+64 9 801 0034 (Int'l CHEMTREC)

SECTION 2: Hazards identification

2.1 Classification of the substance or mixture

Classification according to Regulation (EC) No 1272/2008
Acute toxicity, Oral (Category 4), H302
Acute toxicity, Dermal (Category 3), H311
Eye irritation (Category 2), H319

For the full text of the H-Statements mentioned in this Section, see Section 16.

Classification according to EU Directives 67/548/EEC or 1999/45/EC
Xn Harmful R21/22, R36

For the full text of the R-phrases mentioned in this Section, see Section 16.

2.2 Label elements

Labelling according Regulation (EC) No 1272/2008
Pictogram

Signal word Danger

Hazard statement(s)
H302 Harmful if swallowed.
H311 Toxic in contact with skin.
H319 Causes serious eye irritation.

SAFETY DATA SHEET

Version 5.11
Revision Date 21.09.2017
Print Date 18.10.2018

1. IDENTIFICATION OF THE SUBSTANCE/MIXTURE AND OF THE COMPANY/UNDERTAKING

1.1 Product identifiers

Product name : Iron(III) chloride

Product Number : 157740
Brand : Sigma-Aldrich

1.2 Other means of identification

Ferric chloride

1.3 Relevant identified uses of the substance or mixture and uses advised against

For R&D use only. Not for pharmaceutical, household or other uses.

1.4 Details of the supplier of the safety data sheet

Company : Sigma-Aldrich New Zealand Co.
PO BOX 106-406
1030 AUCKLAND
NEW ZEALAND

Telephone : 0800 936 666

1.5 Emergency telephone number

Emergency Phone # : 0800 928 888 (NZ)
+64 9 801 0034 (Int'l CHEMTREC)

2. HAZARDS IDENTIFICATION

2.1 GHS Classification

Acute toxicity, Oral (Category D)
Skin irritation (Category A)
Serious eye damage (Category A)
Aquatic toxicity (Acute or Chronic) (Category B)

2.2 GHS Label elements, including precautionary statements

Pictogram

Signal word Danger

Hazard statement(s)
H302 Harmful if swallowed.
H315 Causes skin irritation.
H318 Causes serious eye damage.
H411 Toxic to aquatic life with long lasting effects.

Precautionary statement(s)

Prevention
P264 Wash skin thoroughly after handling.
P270 Do not eat, drink or smoke when using this product.

SAFETY DATA SHEET

Version 5.3
Revision Date 07.08.2018
Print Date 18.10.2018

1. IDENTIFICATION OF THE SUBSTANCE/MIXTURE AND OF THE COMPANY/UNDERTAKING

1.1 Product identifiers

Product name : Zinc oxide

Product Number : 544906
Brand : Aldrich

1.2 Other means of identification

No data available

1.3 Relevant identified uses of the substance or mixture and uses advised against

For R&D use only. Not for pharmaceutical, household or other uses.

1.4 Details of the supplier of the safety data sheet

Company : Sigma-Aldrich New Zealand Co.
PO BOX 106-406
1030 AUCKLAND
NEW ZEALAND

Telephone : 0800 936 666

1.5 Emergency telephone number

Emergency Phone # : 0800 928 888 (NZ)
+64 9 801 0034 (Int'l CHEMTREC)

2. HAZARDS IDENTIFICATION

2.1 GHS Classification

Skin irritation (Category B)
Eye irritation (Category A)
Aquatic toxicity (Acute or Chronic) (Category A)

2.2 GHS Label elements, including precautionary statements

Pictogram

Signal word Warning

Hazard statement(s)
H316 Causes mild skin irritation.
H320 Causes eye irritation.
H400 Very toxic to aquatic life.

Precautionary statement(s)

Prevention
P264 Wash skin thoroughly after handling.
P273 Avoid release to the environment.

Response
P305 + P351 + P338 IF IN EYES: Rinse cautiously with water for several minutes. Remove

CHEMMAT 751 A/B - PROJECT COMPLETION SIGN OFF – LABORATORY USE

(The completion of this section is required before your final mark is processed. Scan and attach the completed form to your Appendix section of your final report)

Name of Student: Ellie McBurney

Research Project Title: Photocatalysis using semi-conducting polymers for wastewater...

Supervisor's name: Alisyn Nedoma

List the labs used for this project: 333, CE labs

(If you did not use any of the department labs, simply write 'NA' and obtain your supervisor's signature)

Lab Room(s)	Name of PIC	Area Left Tidy? (Y/N/NA)	Equipment dismantled/returned? (Y/N/NA)	Chemicals handover/disposed safely? (Y/N/NA)	PIC signature
333	AN	Y	Y	Y	Alisyn J. Nedoma

Supervisor's signature: Alisyn J. Nedoma

(Note to Supervisors: Please ensure the student has correctly included ALL the lab facilities used)